Cell. Mol. Life Sci. (2016) 73:3599–3621
DOI 10.1007/s00018-016-2183-4

Cellular and Molecular Life Sciences

ORIGINAL ARTICLE

CASK stabilizes neurexin and links it to liprin-α in a neuronal activity-dependent manner

Leslie E. W. LaConte[1] · Vrushali Chavan[1] · Chen Liang[1] · Jeffery Willis[1] · Eva-Maria Schönhense[3] · Susanne Schoch[3] · Konark Mukherjee[1,2]

Received: 9 October 2015 / Revised: 23 February 2016 / Accepted: 14 March 2016 / Published online: 25 March 2016

Abstract CASK, a MAGUK family protein, is an essential protein present in the presynaptic compartment. CASK's cellular role is unknown, but it interacts with multiple proteins important for synapse formation and function, including neurexin, liprin-α, and Mint1. CASK phosphorylates neurexin in a divalent ion-sensitive manner, although the functional relevance of this activity is unclear. Here we find that liprin-α and Mint1 compete for direct binding to CASK, but neurexin1β eliminates this competition, and all four proteins form a complex. We describe a novel mode of interaction between liprin-α and CASK when CASK is bound to neurexin1β. We show that CASK phosphorylates neurexin, modulating the interaction of liprin-α with the CASK–neurexin1β–Mint1 complex. Thus, CASK creates a regulatory and structural link between the presynaptic adhesion molecule neurexin and active zone organizer, liprin-α. In neuronal culture, CASK appears to regulate the stability of neurexin by linking it with this multi-protein presynaptic active zone complex.

Keywords Synapse · Protein–protein interaction · Protein phosphorylation · Protein complex · Neuron · Mint1 · Active zone · Protein turnover

Introduction

Presynaptic active zones, which are morphologically defined as electron dense projections on the cytosolic surface of the synaptic plasma membrane [1], are the sites of neurotransmitter release. Several multidomain scaffolding proteins which presumably organize the formation or function of active zones have been described in the literature [2]. CASK was one of the first such scaffolding molecules to be identified due to its ability to bind the cytosolic tail of the presynaptic adhesion molecule neurexin [3]. Deletion of CASK does not directly alter the structure of the active zone [4], indicating that CASK may play a regulatory role at the presynapse rather than acting as a structural organizer. Consistent with this notion, we have previously shown that CASK phosphorylates the cytosolic tail of neurexin in a synaptic activity-regulated manner [5].

Another family of proteins present at the presynaptic active zone is the liprin-α family (of which there are four mammalian isoforms) [6, 7]. Deletion of liprin-α alters the morphology of the active zone in both worms and flies, strongly suggesting that liprin-α is an evolutionarily conserved active zone organizer [8, 9]. CASK has been shown to interact with liprin-α specifically in vertebrates [10], therefore it is intriguing to consider the idea that the CASK–liprin-α interaction regulates active zone organization specifically in vertebrates. Both CASK and liprins-α are comprised of several domains. A co-crystal structure composed of isolated domains of CASK and liprin-α

Electronic supplementary material The online version of this article (doi:10.1007/s00018-016-2183-4) contains supplementary material, which is available to authorized users.

✉ Konark Mukherjee
konark@vtc.vt.edu

[1] Virginia Tech Carilion Research Institute, 2 Riverside Cir., Roanoke, VA 24016, USA

[2] Department of Biological Sciences, Virginia Tech, Blacksburg, VA 24060, USA

[3] Institute of Neuropathology, Sigmund Freud Strasse 25, 53105 Bonn, Germany

suggest that the interaction between these two proteins requires only CASK's CaMK domain [10], and this interaction is purportedly specific to CASK and liprins-α2, 3 and 4 due to the presence of an evolutionarily new loop between liprin's SAM1 and SAM2 domains. When the CASK–liprin-α interaction was first described [11], however, it was concluded that CASK's interaction with liprin-α required both CASK's CAMK domain and its first L27 domain, a binding mode distinct from that described in the crystal structure [10]. Subsequent studies have also suggested the involvement of more than just CASK's CaMK domain in its interaction with liprin-α [12].

The physiological existence of the CASK–liprin-α complex has also been difficult to confirm. Several lines of biochemical evidence, including mass spectrometry and affinity chromatography, suggest that the CASK–liprin-α complex may not be constitutively present in the brain [13, 14]. Intriguingly, a close examination of the CASK–liprin-α crystal structure [10] provides a structurally-based hypothesis for why liprin-α might not have been found in these studies. The hydrophobic patch on the surface of CASK's CaMK domain which makes contact with a loop of liprin-α is the same site where other proteins such as Caskin and Mint1 bind to CASK [15], suggesting that liprin-α, Caskin, and Mint1 might compete for binding to CASK's CaMK domain.

The literature describing the interaction of these two important proteins—CASK and liprin-α—is thus contradictory and inconclusive, but this interaction likely has important functional consequences. We have therefore undertaken a careful, biochemically-based examination of this interaction. By using a variety of co-immunoprecipitation strategies from both brain lysate and a reconstituted system in cell culture, we have discovered that the CASK–liprin-α interaction is highly sensitive to the presence of two other important presynaptic proteins, neurexin and Mint1. Our results indicate that CASK and liprin-α have two modes of interaction: (1) a binary interaction consistent with the CASK–liprin-α co-crystal structure, in which Mint1 can compete with liprin-α for binding to CASK, and (2) a ternary interaction, in which liprin-α interacts with an integrated surface generated by a CASK–neurexin complex. This latter complex also accommodates the binding of Mint1, providing evidence for the existence of a complex containing four important synaptic proteins which includes liprin-α and Mint1 simultaneously bound to a CASK–neurexin complex. We further demonstrate that the presence of this multi-protein complex is regulated by CASK-mediated phosphorylation of the cytosolic tail of neurexin. Our findings provide a possible mechanism for how CASK's unique kinase activity regulates the formation of a large protein complex that includes several important players of the presynapse.

Materials and methods

PCR and mutagenesis

mRNA was isolated from adult mouse (postnatal day (P) 28, C57BL/6, males) and rat forebrain (P28, Sprague–Dawley, males) and from hippocampal biopsy specimens of pharmacoresistant mesial temporal lobe epilepsy patients (Caucasian patients with chronic mesial TLE who underwent surgical treatment in the Epilepsy Surgery Program at the University of Bonn Medical Center. Informed consent for use of their tissue was obtained from every patient and all procedures were conducted in accordance with the Declaration of Helsinki and approved by the ethics committee of the University of Bonn Medical Center [16]) with a Dynabeads mRNA Direct Micro kit (Invitrogen) according to the manufacturer's protocol, and first-strand cDNA was prepared using RevertAid Reverse Transcriptase (Fermentas). Alternative splicing of exons was analyzed by RT-PCR. PCR samples contained 1× GoTaq buffer (Promega), 2.5 mM $MgCl_2$, 0.1 mM each of dTTP, dATP, dCTP, and dGTP, 0.5 units of GoTaq (Promega), 10 pmol each oligonucleotide primer (Invitrogen), and 1/20 of the synthesized cDNA in a 25-µl volume. The following primers were used: mouse, (1) FW-5′-GCTGGCCATCCAAGAGATAA-3′, (2) REV-5′-GGTTCATGTCCCCATATGCT-3′, (3) FW-5′-GCTGGCCATCCAAGAGATAA-3′, (4) REV-5′-CCACTCGTGGTTCATGTCC-3′, (5) REV-5′-TCGCAAGTCTTTCTTGGTCA-3′; human (1) FW-5′-CACACGAAGAGATGGAAACG-3′, (2) REV-5′-TCCATGAAGTAGCTGCGGTA-3′, (3) REV-5′-AGCATCCTGGCGTCTACAAG-3′, (4) FW-5′-AGGAGATCATGTCGCTGACC-3′, (5) REV-5′-GCGTCTACAAGGCACTCCAT-3′. PCR was performed with conditions as follows: 2 min at 94 °C, then 30 cycles of 45 s at 94 °C, 30 s at 60 °C, and 45 s at 72 °C followed by a final extension step at 72 °C for 10 min. PCR products were analyzed on a 2.5 % agarose gel. A control (no template) was included for each primer set.

For qPCR experiments, RNA was extracted from TTX/APV or DMSO-treated neurons as described above 20 h post-treatment using TriReagent® (Sigma) and treated with DNASE-1 (Fisher Scientific). cDNA was generated using iScript® cDNA synthesis kit (BioRad) for dye-based quantitative PCR using iTaq™ Universal SYBR® Green Supermix (BioRad) on a BioRad® CFX Connect™ real time PCR machine. GAPDH was used as control and primers for neurexin1α and neurexin1-β were used as previously described [17].

Site-directed mutagenesis was performed using PhusionTM polymerase as described previously [18].

Cells, plasmids and antibodies

Human embryonic kidney (HEK293) cells (ATCC) were cultured in DMEM (HyClone™) containing 10 % fetal bovine serum (HyClone™) supplemented with 5 mg/ml penicillin–streptomycin (HyClone™) at 37 °C and 5 % CO_2. GFP-CASK was prepared as previously described [18]. Rat liprin-α3 was cloned into the *Bgl*II site downstream of dsRED. pCMV-Mint1 is a kind gift from Dr. Südhof. For pulldown assays and immunoblots, cells were plated in 6-well plates and transfected at 80 % confluency with 2 μg of indicated DNA per well using calcium phosphate as described [19]. Six hours post-transfection, fresh media was exchanged.

Liprin-α isoform specific antibodies used were previously described [20]. Liprin-α3 antibody 4396 was a kind gift from Dr. Südhof and was used at 1:4000 for immunoblotting. The CASK antibody (anti-CASK scaffolding protein, cat. no. #75-000) was purchased from Antibodies, Inc., and used for immunoprecipitation at 1:100. The monoclonal bassoon antibody was purchased from Enzo Life Sciences (cat. no. ADI-VAM-PS003-F) and diluted 1:100 for immunostaining. The anti-pan-neurexin-1 polyclonal antibody (ABN161) was purchased from Millipore and used at 1:1000 for western blots and 1:100 for immunostaining, anti neurexin-1α antibody (ABN35) was also bought from Millipore and used at 1:1000 for western blots. To characterize the neurexin antibody, cells expressing neurexin-1β-mCherry were immunolabeled; the staining indicated specificity for HEK cells transfected with neurexins (data not shown). We also performed a modified antigen blocking experiment; briefly, diluted antibodies were incubated with either agarose beads with only GST or with GST-neurexin cytosolic tail. This mixture was then spun down, and supernatant was used for immunostaining neuronal culture. The antibody incubated with GST produced predominantly an axonal staining pattern since it poorly co-localized with dendritic marker MAP2 (Online Resource 1), but no staining was observed with the antibody incubated with neurexin cytosolic tail (data not shown).

Pull-down assays from brain lysate

All animal tissues were obtained under an IACUC protocol approved by Virginia Tech. Brains from male and female C57BL/6J mice between the ages of 5 weeks and 5 months or from male and female Long-Evans rats between the ages of 3 and 4 months were homogenized with a Dounce homogenizer in PBS (phosphate buffered saline) containing protease inhibitors (0.1 mg/ml aprotinin, 0.1 mg/ml leupeptin, 0.1 mg/ml pepstatin, and 0.01 mg/ml PMSF; all purchased from Fisher Scientific), 2 mM EDTA and 5 mM DTT. Homogenates were centrifuged for 30 min at 15,000 rpm at 4 °C to collect membranous fraction. The membrane pellet was washed two times with above buffer and solubilized by the addition of Triton X-100 (final concentration, 1 %) and rocking at 4 °C for 2 h. The insoluble fraction was then pelleted at 30,000*g* for 15 min and supernatant was filtered through a 0.45 μm syringe filter (GE® Whatman, PURADISC™, cat. no. 6746-2502). Supernatant was precleared with 25 μl of protein A/G beads to get rid of endogenous antibodies. CASK antibody (10 μl) was then added to the preclarified brain lysate and incubated overnight at 4 °C with rocking to allow complex formation. Protein A/G beads (Pierce) were washed and 25 μl of beads were then added for 1 h at 4 °C to precipitate the immune complex. The beads were washed three times in PBS + 10 % Triton X, 20 μl of 2× sample buffer was added and boiled for 10 min prior to immunoblotting (see below). For GST-fusion protein pull-downs, the filtered brain lysate, prepared as above, was pre-cleared overnight with rocking at 4 °C with 30 μl glutathione agarose beads (Pierce) for 3 ml of mouse brain homogenate. The filtrate was incubated with 5–10 μg of the indicated GST-fusion protein beads for 2 h at 4 °C. The beads were washed three times with PBS with 1 % Triton X-100 and 30 μl of 2× SDS sample buffer was added to the beads and boiled. For experiments done in the presence or absence of ATP, after pre-clearing as described above, 1 ml of brain lysate in K-Glu buffer (120 mM potassium glutamate, 20 mM potassium acetate, 2 mM EGTA, and 20 mM HEPES–NaOH, pH 7.4) with protease inhibitors (aprotinin, leupeptin, pepstatin, PMSF) and phosphatase inhibitor cocktail 2 and 3 (Sigma) was incubated for 2 h at room temperature with 10 μl GST-CASK beads either in the presence of 5 mM $MgCl_2$ to inhibit CASK kinase activity or in the presence of 5 mM EDTA and 10 mM ATP to activate CASK kinase activity. The beads were washed three times with K-Glu buffer with 1 % Triton X-100 and 20 μl of 2× SDS sample buffer was added to the beads and boiled.

Phosphorylation assay

To demonstrate neurexin phosphorylation, pull-down assays using brain lysate were performed as above, with buffer spiked with 1 microcurie of ATP[γ-^{32}P] (PerkinElmer, cat. no. NEG002A250UC).

Pull-down assays from HEK293 cells

HEK293 cells were transiently transfected with plasmids of interest using calcium phosphate [19]. Two days later cells were harvested and solubilized in PBS containing 1 % Triton-X-100, 2 mM EDTA and protease inhibitors

(aprotinin, leupeptin, pepstatin, PMSF). The lysate was centrifuged at 30,000 rpm. Beads were added to lysate as follows depending upon the pull-down strategy of interest. GFP-trap™ beads (5 µl per reaction) were added to the lysate for 1 h at 4 °C to capture GFP-CASK or the indicated GST-fusion protein agarose beads (5 µg) were added to the lysate for 2 h at 4 °C to capture protein complexes of various composition. For pull-down of the quaternary complex, cell lysate was incubated in the presence or absence of excess purified NxCT (approximately 20 µg/µl) overnight on a rocker at 4 °C, then anti-FLAG M2 Affinity beads (25 µl per reaction; Sigma) were added to the cell lysate for 2 h at 4 °C. Beads were washed three times with TBS (50 mM Tris–HCl, pH 7.4; 150 mM NaCl) and boiled in SDS sample buffer. Protein samples were separated using SDS-PAGE and immunoblotted for specific proteins as described below.

Immunoblots

Proteins were resolved using SDS-PAGE (sample volumes loaded were based on estimates of appropriate protein concentration), transferred to a nitrocellulose membrane (Fisher), and immunoblotted for the proteins of interest. For more quantitative blots, a fluorophore-conjugated secondary antibody was used instead of an HRP-conjugated secondary antibody. The blots were developed using Amersham ECL western blotting detection reagents (GE Healthcare Life Sciences) for HRP secondaries or analyzed for fluorescence directly. All blots were imaged using a ChemiDoc™ MP System (BioRad), and band intensities were quantified using the accompanying ImageLab™ software. Quantifications of the percent of protein pulled down in blots were determined by normalizing the band intensities of the input and pellets bands for volume loaded. In some instances quantities of co-precipitated protein are described as percentages of the primarily precipitated protein.

Triton X-114 phase separation of homogenized mouse brain

Brains from 5-week-old male and female C57BL/6J mice were homogenized as described above. Triton X-114 phase separation protocol was adapted from a previously published protocol [21]; 4 % Triton X-114 (Sigma) was made in PBS containing protease inhibitors and mixed 1:1 with brain homogenate. The sample was first incubated on ice for 10 min and then incubated at 37 °C for 10 min to allow the formation of two phases. The sample was then centrifuged at 25 °C for 10 min at 13,000*g* for final phase separation (aqueous phase on top, a detergent phase in the middle, and a pellet at the bottom). The aqueous phase was then subjected to linear glycerol gradient centrifugation, as described below.

Linear glycerol gradient centrifugation

A linear glycerol gradient (10–40 %) buffer was made using a Gradient Master™ (BioComp Instruments, Inc.) containing 25 mM HEPES–NaOH, pH 7.2, 150 mM NaCl, 5 mM DTT, 2 mM EDTA and protease inhibitors as described above. 10 ml of linear glycerol gradient buffer was loaded in ultracentrifuge tubes used with SW41 Ti Rotor (Beckman Coulter). Sample (0.5 ml of the aqueous phase from the Triton X-114 phase separation of homogenized brain) was carefully layered on top of the gradient buffer and then centrifuged for 20 h, at 35,000 rpm at 4 °C. A total of 9 fractions (1.1 ml each) were collected using the Piston Gradient Fractionator (BioComp Instruments, Inc.) for SDS-PAGE.

Purification of recombinant CASK

CASK protein with an N-terminal GST tag and a C-terminal 6-His-tag was expressed in *E. coli*. Bacterial pellet was lysed using lysozyme and sonication, and CASK was affinity-purified using HisPur Ni-NTA resin (ThermoFisher Scientific). GST-tag was removed by thrombin cleavage while protein was attached to resin, and purified CASK was eluted with 300 mM imidazole.

Recruitment assays

HEK293 cells were plated on 50 µg/ml poly-L-lysine (Sigma Aldrich Inc.)-coated coverslips (12-545-80 microscope coverglass; Fisherbrand, Inc.) in 24-well plates (JetBiofil) and co-transfected with 0.25 µg EGFP-CASK DNA in the pEGFP-C3 vector, 0.25 µg FLAG-tagged neurexin-1β DNA in the pCMV vector and 0.25 µg ds-RED-liprin-α3 DNA using calcium phosphate [19]. Two days post-transfection, the cells were washed in PBS and fixed with 4 % paraformaldehyde in PBS at room temperature for 20 min. Cells were permeabilized using PBS with 0.01 % Triton-X 100 solution and blocked using 5 % fetal bovine serum. Cells were immunostained using monoclonal anti-FLAG antibody (1:100) followed by Alexa-633 (1:250) anti-mouse antibody. Coverslips were mounted on microscope slides (Premiere) using Vectashield (Vector Laboratories Inc.) and visualized using confocal laser scanning microscopy (ZEISS Axio Examiner.Z1 LSM 710) at room temperature with sequential scanning. Images were acquired using Zeiss ZEN 2011 acquisition software. Colocalization was quantified by using the Image Correlation Analysis plugin of ImageJ.

Values of Mander's overlap coefficient (*R*) were reported as percent colocalization.

Computational modeling

Molecular visualization, editing and analysis were done and publication images were produced using the UCSF Chimera package [22]. To model the binding of Mint1 to CASK, coordinates from the crystal structure of the liprin-α/CASK complex [10], 3TAC.pdb, were used as a template. Residues critical for the CASK/liprin interaction were identified as Val980, Trp981, and Val982 in liprin-α [10]. A short sequence from Mint1 (residues 369–400 of the mouse Mint1 sequence, accession number B2RUJ5.2) containing Mint's putative CASK-interacting domain [15], including the three residues (Ile383, Trp384, and Val385) identified to be the binding motif complementary to that identified in liprin, was used as the target sequence for building a homology model using the Modeller module [23] built into Chimera. Ten models were generated by Modeller, and the model that showed the best overlap in the region of the binding motif (lowest RMSD) was selected for further refinement. Loop refinement on all residues except the binding motif (IWV) was next done on the selected model using the Modeller module of Chimera, excluding the three binding motif residues. The standard loop modeling protocol was used. The model chosen for further analysis and included in the figure (Fig. 1a, b) was selected based on high GA341 score, low zDOPE score, overlap between liprin-α and Mint1 of the three binding motif residues, and no clashes with CASK. To model the CASK V117E mutant, Chimera's Rotamers structure editing tool was used to modify 3TAC.pdb. Rotamer for introduced glutamate was chosen from the Dunbrack backbone-dependent rotamer library [24] based on preferred orientation for forming a salt bridge with R106. R106 was also modified using the rotamer library to select an orientation favoring salt bridge formation. Energy minimization using default settings in Chimera was performed, fixing all atoms except those within a 10 Å radius of V117E. The salt bridge was identified and visualized using Chimera's FindHbond tool.

Neuronal culture

Neuronal cultures were made from pups in which all cortical neurons were specifically labeled with tdTomato (described in [25]). Cortices from newborn pups (postnatal day 1.5) were dissected and isolated in ice-cold Hank's balanced salt solution. The cortices were minced and digested with 0.25 % trypsin for 5 min at 37 °C. Trypsin was inactivated by using complete DMEM media (as described above). Digested pieces of cortices were then triturated using a Pasteur pipette and filtered through a 100 μm nylon cell strainer (Corning, cat. no. 431752). Filtered cells were centrifuged at 400*g* for 5 min room temperature. The cell pellet was resuspended in complete neuronal media and plated on polylysine coated coverslips. The neurons were maintained in neuronal media (Lonza PNGM^{TM} SingleQuots, cat. no. CC-4462 and PNBM media). DIV (days in vitro) eight neurons were either treated with vehicle (DMSO) or 0.5 μM tetrodotoxin (TTX) and 50 μM (2R)-amino-5-phosphonovaleric acid (APV) overnight (20 h) to silence all activity. Coverslips with cultured neurons were washed, fixed with 4 % paraformaldehyde and immunostained with the neurexin and bassoon antibodies for microscopy as described above. Images were analyzed in Fiji to assess neurexin immunostaining; stretches of neurites approximately 200 μm from each quadrant of an image were traced using the freehand tool and mean pixel intensity along the traced line was measured. Ten images from three independent experiments were analyzed.

To generate pups where CASK is specifically deleted in neurons, CASK^{floxed} mice were crossed with Synapsin-Cre [26] mice, and neuronal cultures were generated from CASK knockout P1 pups as described above. Neuronal cultures were transduced on DIV 4 with wildtype CASK and CASK^{4M} (CASK containing the mutations P22A, H145E, C146N, and G162D; [18]) using lentiviral delivery. Neurons were lysed in sample buffer on DIV 9, and immunoblotting assay was performed on the antigens indicated.

Lentiviral production

CASK wildtype or CASK^{4M} cDNA was cloned into a lentiviral shuttle vector (third generation), and lentiviral particles were generated following the protocol described by Tiscornia et al. [27]. Briefly, HEK 293 cells were transfected using CASK vectors and the packaging vectors. Forty-eight hours later, the supernatant was ultracentrifuged to obtain concentrated lentiviral particles. Viral titers were tested on HEK 293 cells.

Results

All liprins-α and Mint1 contain a homologous loop that interacts with CASK

CASK, as a putative scaffolding protein, is known to have many binding partners, but the specific structural interactions with those binding partners have been difficult to define. The co-crystal structure of CASK and liprin-α2 [10] offers insight into one such interaction, but also elicits

further questions when looked at in the context of previous work. The co-crystal structure, composed of CASK's CaMK domain and liprin-α2's three SAM domains, suggests that the CaMK domain of CASK is sufficient for the binding of liprin-α to CASK. In the crystal structure, liprin's interaction with CASK is mediated by all three SAM domains of liprin-α, with a particularly important role played by a purportedly vertebrate-specific loop between the SAM1 and SAM2 domains [10]. This loop contains a VWV (valine-tryptophan-valine) motif [10] (Fig. 1a) and is encoded by an exon subjected to alternate splicing [28], leading to speculation that this insertion was acquired more recently in evolution [10]. The importance of this alternatively spliced loop in the CASK–liprin interaction led to the conclusion that one of the liprin isoforms, liprin-α1, is not a natural binding partner for CASK [10] because it was thought that this loop was absent from liprin-α1 in vertebrates. Surprisingly, when examining the genomic sequences from various mammals, we found that liprin-α1 does indeed contain the region encoding this particular loop (Fig. 1a shows both known and predicted protein sequences based on genome analysis). The reference sequence for mouse liprin-α1 mRNA (NM001033319) includes the VWV-containing loop (Fig. 1a) and is subject to alternative splicing [28].

To determine if alternative splice variants of liprin-α1 from other mammals also contain this loop, we performed RT-PCR on mouse, rat and human cDNA using either primers flanking exon 24, which codes for the VWV-containing loop (Fig. 1b, middle and right lanes of both gels; rat data in Online Resource 2) or with forward primer located on the VWV-encoding exon (Fig. 1b, both gels, left lanes). Sequencing of the PCR products confirmed that splice variants of liprin-α1 containing this loop do exist in mouse and human (Fig. 1b), and the isoform containing the VWV motif is expressed across a number of brain regions in mouse (Fig. 1c). Indeed, sequence analysis suggests that this loop is present outside the vertebrate clade in animals such as *Ciona intestinalis,* indicating that, in fact, the sequence originated before the emergence of vertebrates (Fig. 1a).

In the CASK–liprin co-crystal structure, the central tryptophan of liprin's VWV motif is buried in a hydrophobic pocket formed by V117, Y113, I103, and Y121 of the CASK CaMK domain (Fig. 1d, e). Interestingly, this same evolutionarily conserved hydrophobic region of the CaMK domain of CASK has been proposed to be required for interactions with other proteins, including Mint1 and Caskin [15]. Mutating CASK's V117 to either aspartate or glutamate eliminates the interaction of CASK with Caskin, Mint1 and liprin-α [10, 15]. The possibility that liprin-α and Mint1 interact with the same region of the CASK CaMK domain led us to hypothesize that, just as it does with Caskin [14], Mint1 competes with liprin-α for interaction with CASK. To explore the structural feasibility of this idea, we built a homology model of the loop of Mint1 suspected to interact with CASK [15], based on the available co-crystal structure of the CASK–liprin-α2 complex. Thirty-two residues from Mint1 (residues 369–400 from the mouse Mint1 sequence) were aligned with the liprin-α2 residues corresponding to the region identified as interacting with CASK (residues 966–997 of 3TAC.pdb). A series of homology models of Mint1 was calculated, and a representative structure was overlaid on the related liprin-α loop in the CASK–liprin co-crystal structure to approximate a CASK–Mint1 complex (Fig. 1c, d). Parameters of the modeled structure indicate that it is structurally plausible (no clashes with CASK, GA341 score of 0.82 indicating structure is native-like [29]) and that the modeled region of Mint1 could form a loop that would insert into the hydrophobic pocket on CASK in a manner similar to that seen with liprin-α. Of particular interest is the binding motif (VWV) identified in the CASK–liprin co-crystal described above. This region of the co-crystal is shown in detail in Fig. 1e, along with the Mint1 model overlay. In Mint1, the residues corresponding to the binding motif are IWV (Fig. 1a) [15]. The tryptophan residue of both liprin-α and Mint1 inserts into the hydrophobic pocket lined by CASK residues I103, Y113, V117, and Y121 (Fig. 1e). The modeling presented here provides a

Fig. 1 Sequence and structural basis of the CASK–liprin interaction. ▶ **a** Alignment constructed using ClustalW of the sequence of the VWV-containing loop (in *green*) of liprin-α isoforms from different organisms. Sequence accession numbers of aligned sequences are, in order, NP_796008.2, XP_005227322.1, XP_421074.4, XP_006230777.1, XP_006718778.1, F6ZZL8, NP_001207403.1, NP001192270.1, NP_003651.1, and NP_084017.2. Sequences beginning with "XP" indicate model sequences determined from genomic computational analysis by NCBI. In *red* is shown the VWV motif predicted to insert into a hydrophobic pocket in CASK. The alignment of the Mint1 sequence (NP_796008.2) used to construct the homology model of Mint1's interaction with CASK is also shown (residues used in structure calculation are in *purple*). **b** RT-PCR of mouse forebrain and human hippocampus (two replicates per species). Primers 1 and 2 for both mouse and human cDNA were located in exon 24 (contains the VWV-containing loop) and the adjacent exon; primers 3 and 4 or 5 flank all three exons of interest (23, 24, and 25). PCR products confirm the existence of splice variants containing the VWV-containing loop in liprin-α1 cDNA. *M* 100 bp ladder; *arrows* indicate PCR products that were sequenced (predicted peptide sequence shown). **c** RT-PCR of mouse brain regions as specified, using primers that flank the VWV-containing exon. *Arrows* indicate bands from products that contain exon 24 with the VWV motif. **d** Co-crystal structure (3TAC.pdb) of CASK (*brown*) and liprin-α (*green*), with homology model of Mint1 (*lavender*) overlaid on liprin-α. **e** Hydrophobic binding pocket of CASK with binding motifs of liprin-α (*green*) and Mint1 (*lavender*). Central tryptophan of the VWV binding motif (W980 for liprin, W384 for Mint1) is labeled TRP. Residues forming CASK's hydrophobic binding pocket are shown in *yellow*, with critical valine residue in *red*

a

VWV-containing loop

Liprin-α1	M.musculus	SPSAPPTSRTTTGNVWLTHEEMETLT-ATPQTEDEEGSWAQ-------TLAYGDMNHE
	B.taurus	SPSAPPTSRTTTGNVWLTHEEMETLT-ATPHTEDEEGSWAQ-------TLAYGDMNHE
	G.gallus	SPSAPPTSRTTTGNVWVTHEEMENLT-ASQQT----------------TLAYGDMNHE
	R.norvegicus	SPSAPPTSRTTTGNVWLTHEEMETLT-ATPQTEDEEGSWAQ-------TLAYGDMNHE
	H.sapiens	SPSAPPTSRTTTGNVWLTHEEMETL-AATPQTEDEEGSWAQ-------TLAYGDMNHE
	C.intestinalis	SPSAPPTSRTTTGSVWMTHEEVDSLTNQIPLTDDEAG-WAEMCFVISQTLAYGDMNHE
Liprin-α2	H.sapiens	SPSAPPTSRTPSGNVWVTHEEMENLAAPAKTKESEEGSWAQ-CPVFLQTLAYGDMNHE
	M. musculus	SPSAPPTSRTPSGNVWVTHEEMENLTAPAKTKESEEGSWAQ-CPVFLQTLAYGDMNHE
Liprin-α3	H.sapiens	SPSAPASSRTSTGNVWMTHEEMESLTATTKP-ETKEISWEQ-------TLAYGDMNHE
	M. musculus	SPSAPASSRTPTGNVWMTHEEMESLTAATKP-ETKEISWEQ-------ILAYGDMNHE
Mint1	M.musculus	TIRSPYTPDEPKEPIWVMRQDI-SPTRDCDDQRPVDGDSPSPGSSSPLGAESSSIPLH

b

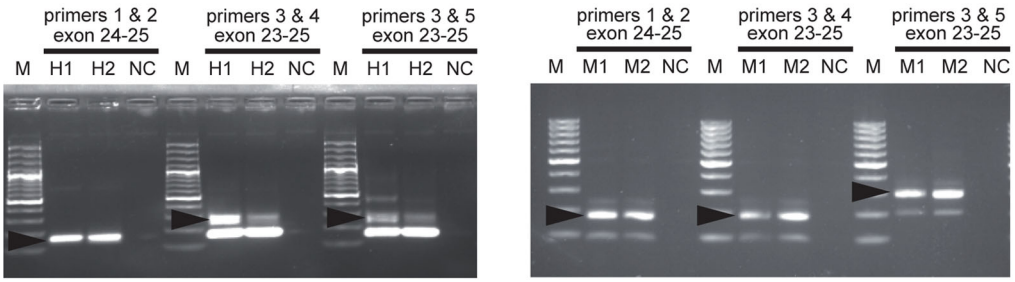

Human peptide: TTGNVWLTHEEMETLAATPQTEDEEGSWAQ
Murine peptide: TTGNVWLTHEEMETLTATPQTEDEEGSWAQ

c

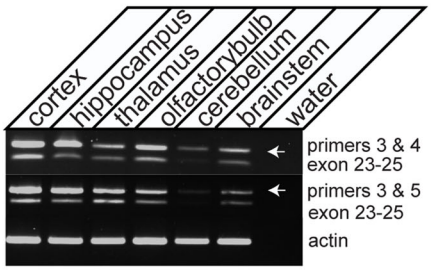

d

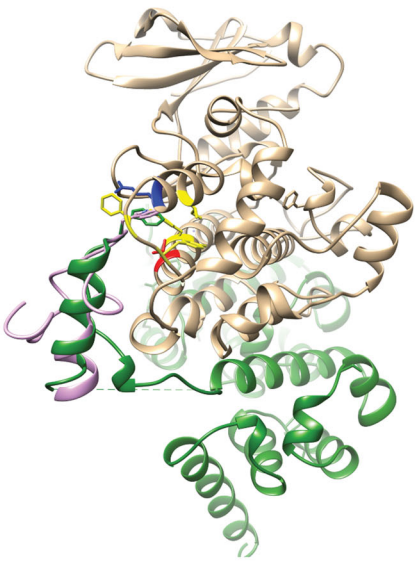

e

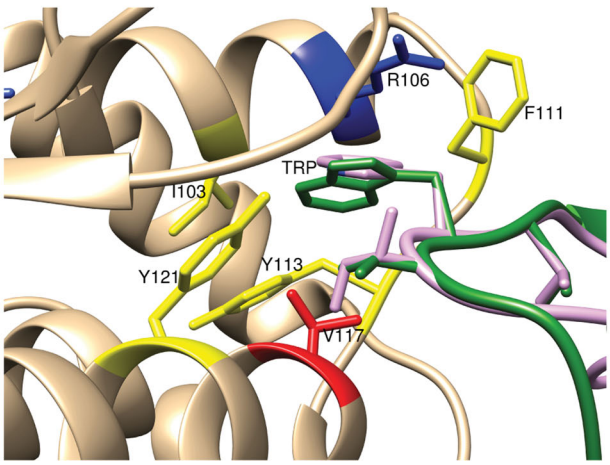

structural basis for the binding of Mint1 to CASK, supporting the possibility that Mint1 competes with the homologous loop in liprin-α to displace liprin-α from CASK.

Mint1 inhibits the interaction between CASK's CaMK domain and liprins-α

Early studies aimed at finding protein binding partners of CASK failed to identify liprin-α as a potential interactor [13, 14]. Immunoprecipitation of CASK using a CASK antibody resulted in co-precipitation of stoichiometric amounts of Mint1 and a few peptides of Caskin, suggesting that Mint1 is the predominant binding partner of CASK's CaMK domain in the brain [13, 14]. This endogenous Mint1–CASK interaction has also been demonstrated in *C. elegans*, and we have recently confirmed it in Drosophila, indicating that the CASK–Mint1 interaction is evolutionarily conserved [30]. Similarly, affinity chromatography using the CaMK domain of CASK identified Mint1, Caskin and Nedd4 as potential CASK binding partners. The contradiction between the many immunoprecipitation studies which fail to reveal the CASK–liprin interaction and the crystal structure that demonstrates a clear structural basis for a CASK–liprin interaction led us to explore the possibility that Mint1 and liprin-α compete for CASK's CaMK domain under physiological conditions. To do this, we first performed a CASK immunoprecipitation experiment from whole mouse brain homogenate using a CASK antibody whose epitope consists of CASK's L27 domains (Fig. 2a). Consistent with previous findings, our results indicate that Mint1 co-precipitates efficiently with CASK, whereas liprin-α does not (Fig. 2b). We next performed immunoprecipitation experiments from cells transfected with combinations of GFP-CASK, liprin-α, and Mint1, allowing us to use GFP as an external epitope of CASK to avoid any complications that might arise due steric hindrance with an internal epitope, such as CASK's L27 domains. Co-transfections of HEK293 cells with GFP-CASK and either Mint1 or liprin-α3 or both Mint1 and liprin-α3 were performed to test these protein–protein interactions biochemically. Two days after transfection, GFP-trap beads® were used to immunoprecipitate GFP-CASK (Fig. 2c). Neither liprin-α3 nor Mint1 binds independently to these beads, confirming the specificity of the beads for only GFP-fusion proteins. GFP-trap beads® efficiently pulled down GFP-CASK, and when co-expressed with CASK individually, both liprin-α3 and Mint1 robustly immunoprecipitate with CASK (Fig. 2c), which is consistent with earlier studies and indicates that both proteins are capable of interacting with GFP-CASK in HEK293 cells. When all three proteins (GFP-CASK, Mint1 and liprin-α3) are co-expressed, only Mint1 is co-precipitated (Fig. 2c, d), indicating that Mint1 and liprin-α compete for binding to GFP-CASK. Our data therefore suggest that in the presence of Mint1, liprin-α competes for the same binding site on CASK.

Previous work showed that in a GST-pulldown assay from brain lysate that used CASK's CAMK domain as bait, only Caskin, Mint1 and Nedd4 were precipitated, but not liprin-α [14]. To follow up on the domain specificity of the CASK–liprin interaction, we compared the ability of full-length CASK (GST-tagged) and CASK's isolated CaMK domain (also GST-tagged) to pull down liprin-α (Fig. 2e, f) from brain lysate. Our data indicate that full-length CASK can pull down liprin-α more effectively than the CaMK domain alone, suggesting that the isolated CaMK domain may not be the ideal binding partner for liprin-α in the presence of other interacting proteins like Mint1 and Caskin. Importantly, it also suggests that, under physiological conditions, the CASK–liprin-α interaction may involve additional domains of CASK. This is corroborated by a previous study [11], in which it was determined that all liprin-α isoforms (1, 2, 3, and 4) interact with a CASK region that encompasses the CaMK domain and the L27 domain. It has also been shown that the CASK–liprin-α

Fig. 2 Mint1 competes with liprin-α for CASK interaction. **a** Domain structure of CASK showing the regions included in the GST-CaMK and GST-CASK constructs. CASK antibody used in immunoprecipitation was raised against L27 motifs. **b** CASK antibody was used to immunoprecipitate CASK and binding partners from mouse brain lysate. A cartoon diagram representing the immunoprecipitation experiment is shown *below* the *panel*. Starting material is shown on the *left* of the *arrow* and predominant species pulled down is shown on the *right* of the *arrow*. CASK, *red*; Mint1, *purple*. **c** HEK293 cells were transiently transfected with cDNAs for GFP-CASK, liprin-α3, or FLAG-tagged Mint1, as indicated. GFP-CASK was precipitated from solubilized cells using GFP-trap™ beads, along with any other interacting proteins, and blots were performed with indicated antibodies. Cartoon diagrams representing the pulldown experiment is shown to the *right* of the *panel*. Starting material is shown on the *left* of the *arrow* and predominant species pulled down is shown on the *right* of the *arrow*. CASK, *red*; Mint1, *purple*; liprin-α, *green*. **d** Quantification of band intensity levels from **c**, showing differences in the percent of input liprin brought down by CASK in the presence or absence of FLAG-Mint1 (mean and SEM; $n = 3$; *asterisk* indicates significance of $p < 0.05$). **e** Glutathione beads bound with either GST-CaMK or GST-CASK (full-length) were used to pull down CASK binding partners from mouse brain lysate. *Left panel* Ponceau S-stained gel demonstrating amounts of sample loaded on gel. *Right panel* blots for indicated proteins (synaptophysin, negative control; neurexin1β, positive control). Cartoon diagrams representing the pulldown experiment is shown to the *right*. Pulldown strategy is indicated by *entity* over the *arrow* (glutathione beads with attached CAMK domain or full-length CASK). Starting material is shown on the *left* of the *arrow* and predominant species pulled down is shown on the *right* of the *arrow*. CASK, both full-length and CAMK domain, *red*; Mint1, *purple*; liprin-α, *green*; neurexin, *blue*. **f** Quantification of band intensity levels from **e** shows differences in the percent of input liprin and neurexin brought down by either full-length CASK or the CAMK domain of CASK (mean and SEM; $n = 3$; *asterisk* indicates significance of $p < 0.05$)

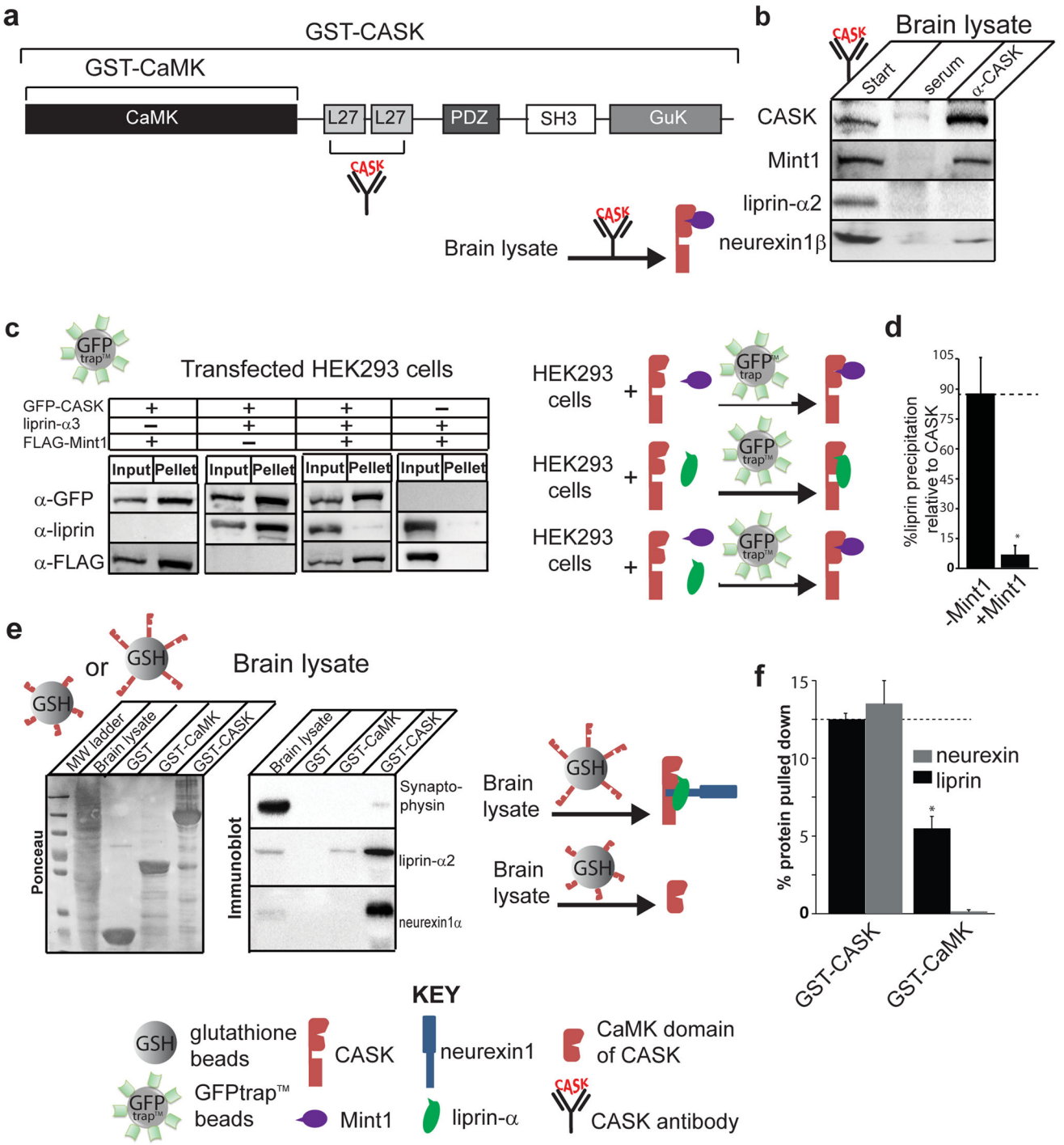
a
GST-CASK
GST-CaMK
CaMK
L27
L27
PDZ
SH3
GuK
CASK
Brain lysate
b
Brain lysate
CASK
Start
serum
α-CASK
CASK
Mint1
liprin-α2
neurexin1β
c
GFP trap
Transfected HEK293 cells
GFP-CASK
liprin-α3
FLAG-Mint1
Input
Pellet
α-GFP
α-liprin
α-FLAG
HEK293 cells
GFP trap
d
%liprin precipitation relative to CASK
105
90
75
60
45
30
15
0
-Mint1
+Mint1
e
or
GSH
Brain lysate
MW ladder
Brain lysate
GST
GST-CaMK
GST-CASK
Ponceau
Immunoblot
Synapto-physin
liprin-α2
neurexin1α
Brain lysate
f
% protein pulled down
15
10
5
0
neurexin
liprin
GST-CASK
GST-CaMK
KEY
glutathione beads
GFPtrap™ beads
CASK
Mint1
neurexin1
liprin-α
CaMK domain of CASK
CASK antibody

interaction is modulated by the CDK5-mediated phosphorylation of two serines in CASK—serine 51 in the CaMK domain and serine 395 in the first L27 domain [12] — highlighting the likely importance of more than just CASK's CaMK domain for liprin-α binding. Since the structural (crystallography) results are at odds with biochemical data in the terms of the domain requirements for the CASK–liprin-α interaction, we sought to further examine this interaction in a cellular context.

CASK and liprin-α form a ternary complex with neurexin at the plasma membrane

Since the CASK–liprin-α interaction may require multiple domains of each protein, we employed a mammalian cell expression system that allows us to express recombinant full-length versions of both liprin-α and CASK. A previously published "recruitment assay" was employed to test protein–protein interaction; the assay is based on a change in the cellular localization of CASK upon co-expression with neurexin. When CASK is expressed in HEK293 cells, it typically distributes in the cytoplasm [5]; when expressed in the presence of the transmembrane protein neurexin-1β, CASK binds to the cytoplasmic tail of neurexin and is recruited to the plasma membrane (Fig. 3b, Online Resource 3). This shift of CASK from mostly cytoplasmic localization to mostly membrane-bound localization is easily observable by confocal microscopy. We reasoned that proteins interacting with CASK will also translocate to the plasma membrane in the presence of neurexin by an indirect "piggy-back" mechanism. Both GFP-CASK (Fig. 3c) and DsRed-liprin-α3 (Fig. 3a) are cytosolic; in contrast, FLAG-tagged neurexin-1β is membrane-bound (Fig. 3). When DsRed-liprin-α3 and GFP are co-expressed with neurexin1β-FLAG (Fig. 3a), DsRed-liprin-α3 remains cytosolic, and GFP partitions between the cytosol and nucleus, indicating that neurexin does not directly interact with either liprin or GFP. When neurexin-1β-FLAG is co-expressed with GFP-CASK, neurexin recruits CASK to the cell membrane (Fig. 3b) as expected, indicating a direct interaction between neurexin and CASK. When all three proteins—liprin-α, CASK, and neurexin-1β—are co-expressed, neurexin-1β-FLAG recruits liprin-α3 to the membrane via CASK (Fig. 3d), clearly confirming the existence of a complex consisting of neurexin-1β, CASK, and liprin- α3 in the HEK293 expression system. Surprisingly, Mint1 co-expression did not convincingly reduce recruitment of liprin-α to the membrane, but instead, both Mint1 and liprin-α3 co-localized with CASK on the membrane (Fig. 3e). This was unexpected, since the immunoprecipitation results indicated that Mint1 outcompetes liprin-α for binding to CASK (Fig. 2c).

Fig. 3 Neurexin recruits CASK and liprin-α to the plasma membrane as a ternary complex. **a–d** HEK293 cells were plated on poly-lysine-coated coverslips and transiently transfected with cDNA for GFP, GFP-CASK, DsRed-liprin-α3, neurexin1β-FLAG or empty vector as indicated. Forty-eight hours later, cells were fixed and immunostained with anti-FLAG primary antibody and anti-mouse-Alexa 633 secondary antibody, mounted on slides, and imaged using laser scanning confocal microscopy at ×63 (*scale bar* is 6 μM). **e** HEK293 cells were plated on poly-lysine-coated coverslips and transiently transfected with GFP-CASK, DsRed-liprin-α3, neurexin1β (without FLAG) and Mint-1-FLAG. Forty-eight hours later, cells were fixed and immunostained with anti-FLAG primary antibody and anti-mouse-Alexa 633 secondary antibody, mounted on slides, and imaged using laser scanning confocal microscopy at ×63 (*scale bar* is 6 μM) ▶

These results led us to hypothesize that CASK and liprin-α must have two modes of interaction—one represented by the CASK–liprin-α crystal structure [10], in which liprin-α binds to CASK via the VWV-containing loop (Fig. 1c, d), and a second binding mode in the presence of neurexin.

The CASK–neurexin complex binds to both liprin-α and Mint1 simultaneously

We further investigated the neurexin–CASK–liprin complex by reconstituting it biochemically. HEK293 cells were transiently transfected with GFP-CASK and either liprin-α3 alone, FLAG-Mint1 alone, or both liprin-α3 and FLAG-Mint1. The GFP–CASK–neurexin complex was reconstituted by precipitating GFP-CASK using the cytosolic tail of neurexin (NxCT) immobilized to glutathione beads via a GST-tag. Interacting proteins were identified by immunoblotting for co-precipitated proteins (Fig. 4a). Not surprisingly, the CASK–neurexin complex interacts with both Mint1 and liprin-α3 in isolation. However, unlike the results seen with CASK co-immunoprecipitation in the absence of NxCT (Fig. 2c), Mint1 did not abolish the interaction between liprin-α3 and CASK; both Mint1 and liprin-α3 co-precipitated with CASK (Fig. 4a, b). One possible mechanism to explain the difference between results obtained with GFP-trap® beads in Fig. 2c and the pull-down assay with GST-NxCT in Fig. 4a could be a direct interaction between neurexin and liprin. Although results from the recruitment assay suggest that neurexin does not directly interact with liprin (Fig. 3a), we further tested this possibility biochemically by using a truncated version of CASK missing the first 162 amino acids of the CaMK domain in the identical pull-down experiment with GST-tagged NxCT (Fig. 4c). Liprin-α3 failed to bind to truncated CASK–neurexin under these conditions, confirming that CASK's CaMK domain is required for the formation of the CASK–neurexin–liprin ternary complex. It is important to note that HEK cells do express native CASK, denoted by the asterisk in Fig. 4c. The presence of

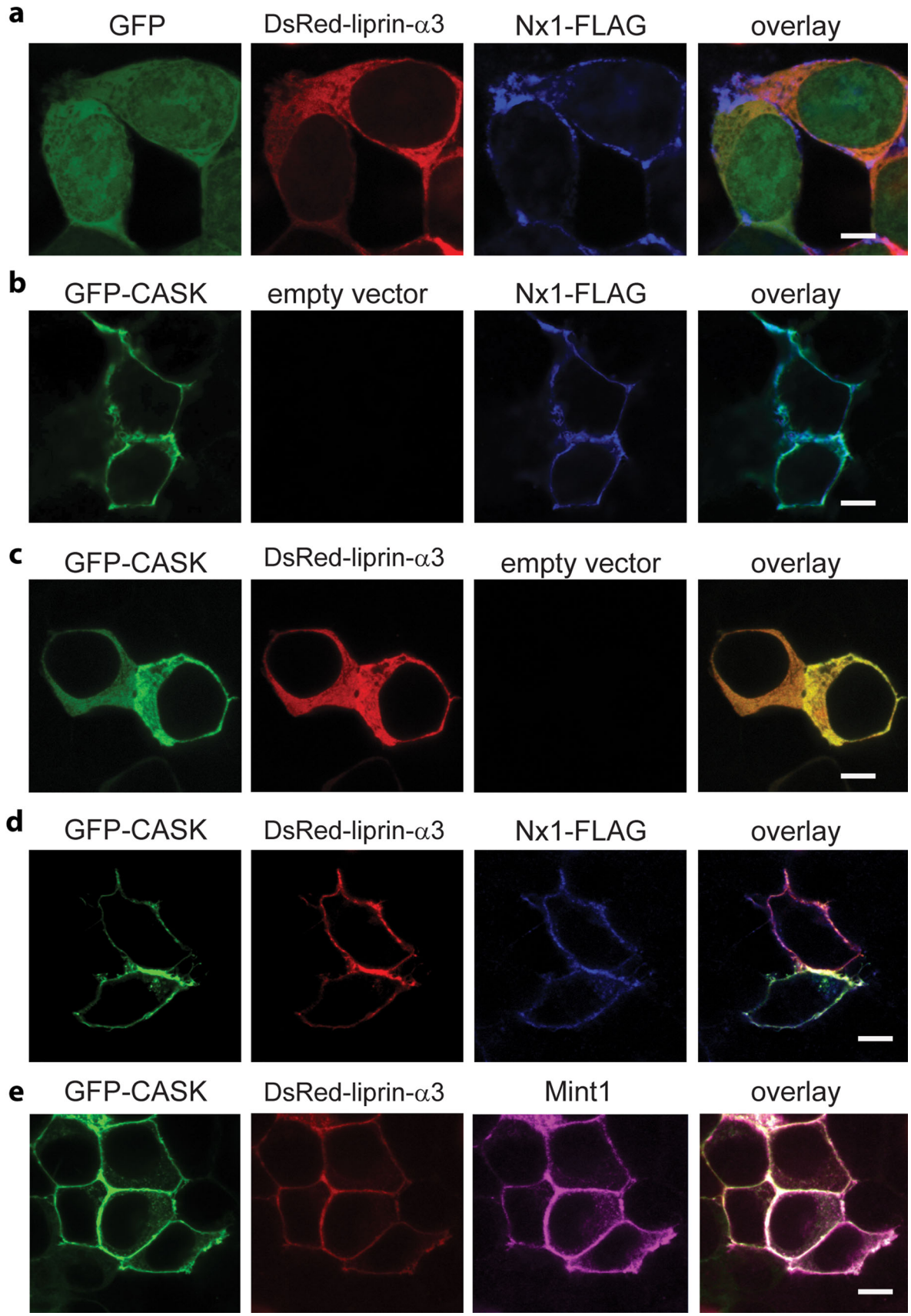
a
GFP
DsRed-liprin-α3
Nx1-FLAG
overlay
b
GFP-CASK
empty vector
Nx1-FLAG
overlay
c
GFP-CASK
DsRed-liprin-α3
empty vector
overlay
d
GFP-CASK
DsRed-liprin-α3
Nx1-FLAG
overlay
e
GFP-CASK
DsRed-liprin-α3
Mint1
overlay

native CASK in HEK cells explains the faint liprin band that appears in samples that come from cells that were not transfected with exogenous CASK.

While our results clearly show that liprin-α binds to CASK in the presence of Mint1 only when CASK is bound to neurexin, the data presented are not capable of distinguishing between two possible scenarios: (1) in the presence of neurexin, the affinity of CASK for liprin-α increases, making liprin-α more competitive with Mint1 for CASK binding, or (2) liprin-α and Mint1 bind to the CASK–neurexin complex simultaneously. To distinguish between these two models, we transiently transfected HEK cells with FLAG-tagged Mint1, GFP-CASK, and DsRed-liprin-α3, collected cell lysate after 48 h and incubated the cell lysate with exogenously expressed GST-NxCT overnight. M2 anti-FLAG affinity gel was then used to pull down FLAG-tagged Mint1 and any associated proteins (Fig. 4d). Indeed, liprin-α3 was found in the immunoprecipitated complex in which neurexin was present, but not when neurexin was absent, confirming the formation of a quaternary complex consisting of CASK, neurexin, Mint1, and liprin-α3. Mint1 and liprin-α therefore do not compete with the same binding site on CASK when CASK is complexed with neurexin, further supporting the idea that there are two modes of interaction between CASK and liprin-α.

To determine whether the CASK–neurexin–liprin-α complex can exist endogenously in the brain, we used the cytoplasmic tail of neurexin to pull down CASK from mouse and rat brain lysate (Fig. 4e, Online Resource 4). The precipitation was specific for CASK since a prominent synaptic protein, synaptophysin, was not pulled down. Precipitated material was blotted for liprin-α isoforms using liprin-α isoform-specific antibodies [20] or for Mint1. In addition to co-precipitating Mint1, CASK co-precipitated all isoforms of liprin-α, including liprin-α1 (Fig. 4e, f), consistent with the findings of Olsen et al. [11]. The pulldown of liprin-α1 was reproducible from rat brain as well (Online Resource 4).

To further define CASK's binding partners in a physiological context, mouse brain homogenate was subjected to phase separation followed by gel filtration. Triton X-114 is widely used to separate integral membrane proteins from peripheral membrane proteins and cytosolic proteins without dissociating tight protein complexes [31]. To characterize endogenous soluble CASK and its protein binding partners, mouse brain homogenate was prepared in Triton X-114 and separated into a detergent-insoluble phase, a detergent phase, and an aqueous phase (Fig. 4g). The aqueous phase, containing soluble CASK, was subjected to centrifugation on a glycerol gradient, along with a sample of purified recombinant CASK for reference. Recombinant CASK was isolated in fraction 2, but CASK from the aqueous phase of brain homogenate was found predominantly in fraction 4, suggesting that in a cellular context, CASK is in complex with itself or another protein (Fig. 4g). When fractions were blotted for liprin-α3 and Mint1, liprin-α3 was found predominantly in fraction 5, whereas most Mint1 was found in fraction 4, the same fraction containing the majority of CASK. These data strongly suggest that liprins-α are not a major cytosolic binding partner of endogenous CASK in brain tissue but that Mint1 is.

Fig. 4 The CASK–neurexin complex binds to both liprin-α and Mint1 simultaneously. **a** HEK293 cells were transiently transfected with cDNA for GFP-CASK, liprin-α, and FLAG-Mint1 as indicated. GFP-CASK was precipitated from solubilized cells using the immobilized GST-tagged cytosolic tail of neurexin and blotted for indicated antigens. The percentage of CASK precipitation in different experiments varied between 12–19 % depending on different lots of GFP-Trap^{TM} beads as well as liprin-α3 co-expression. A cartoon diagram is shown (*right*) representing the experiment performed with immobilized NxCT (*blue*). Starting material is shown on the *left* of the *arrow* and predominant species pulled down is shown on the *right* of the *arrow*. CASK, *red*; Mint1, *purple*; liprin-α, *green*. **b** Quantification of band intensity levels from **a**, showing differences in the percent of input liprin brought down by the CASK complex in the presence or absence of FLAG-Mint1 (mean and SEM; $n = 3$; *asterisk* indicates significance of $p < 0.05$). **c** HEK293 cells were treated as in **a**. t-GFP-CASK is the CASK protein in which the first 162 amino acids have been truncated. HEK293 cells express native CASK, and this band is indicated with an *asterisk* in the far *left lane*. Cartoon diagram (*right*) is shown with truncated CASK, *red*; liprin-α, *green*; and NxCT, *blue*. **d** HEK293 cells were transiently transfected with cDNA for GFP-CASK, liprin-α, and FLAG-Mint1 as indicated. Cell lysate was incubated in the presence or absence of excess purified GST-Nx-CT overnight. Anti-FLAG beads were then used to pull down FLAG-Mint1 and any interacting proteins. Proteins were separated using SDS-PAGE and immunoblotted as indicated. A cartoon diagram is shown (*below*) in which starting material is shown on the *left* of the *arrow* and predominant species pulled down is shown on the *right* of the *arrow*. CASK, *red*; Mint1, *purple*; liprin-α, *green*; NxCT, *blue*. **e** Endogenous CASK protein complex was precipitated from mouse brain with a GST fusion protein of the cytosolic tail of neurexin or with GST alone. Proteins were separated using SDS-PAGE and immunoblotted as indicated. A cartoon diagram (*below*) is shown in which starting material is shown on the *left* of the *arrow* and predominant species pulled down is shown on the *right* of the *arrow*. CASK, *red*; Mint1, *purple*; liprin-α, *green*; NxCT, *blue*. **f** Quantification of band intensity levels from **e**, showing the percent of liprin isoforms or Mint1 present in the brain lysate input brought down by the CASK complex (mean and SEM; $n = 3$). **g** Mouse brain homogenate was subjected to Triton X-114 phase separation. The aqueous phase was then subjected to separation by glycerol gradient (linear, 10–40 %) centrifugation, with recombinant CASK as a reference. Fractions were then run on SDS-PAGE and immunoblotted as indicated. Distributions of proteins across the gradient fractions are shown on the *right*

Mutations that alter the formation of the CASK–liprin-α binary complex do not affect the CASK–neurexin–liprin-α complex

As described above, it has previously been shown that mutating V117 of CASK to E completely abolishes the interaction between CASK and liprin-α or Mint1 [10]. In

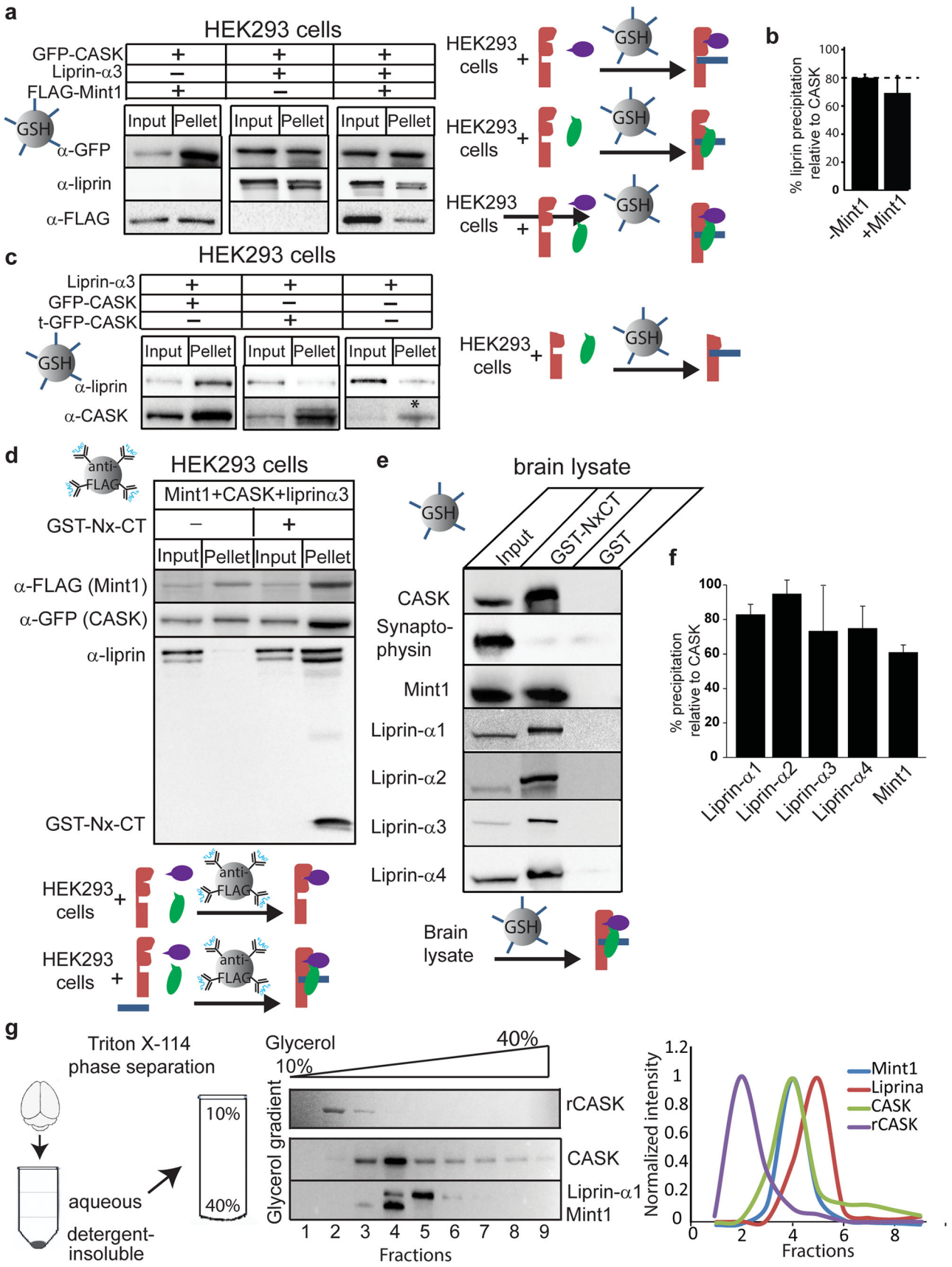
a
HEK293 cells
GFP-CASK
Liprin-α3
FLAG-Mint1
Input
Pellet
GSH
α-GFP
α-liprin
α-FLAG
HEK293 cells
b
% liprin precipitation relative to CASK
-Mint1
+Mint1
c
HEK293 cells
Liprin-α3
GFP-CASK
t-GFP-CASK
α-liprin
α-CASK
d
HEK293 cells
anti-FLAG
Mint1+CASK+liprinα3
GST-Nx-CT
α-FLAG (Mint1)
α-GFP (CASK)
α-liprin
e
brain lysate
Input
GST-NxCT
GST
CASK
Synapto-physin
Mint1
Liprin-α1
Liprin-α2
Liprin-α3
Liprin-α4
Brain lysate
f
% precipitation relative to CASK
Liprin-α1
Liprin-α2
Liprin-α3
Liprin-α4
Mint1
g
Triton X-114 phase separation
aqueous
detergent-insoluble
Glycerol gradient
10%
40%
rCASK
CASK
Liprin-α1
Mint1
Fractions
Normalized intensity
Liprina
CASK
rCASK

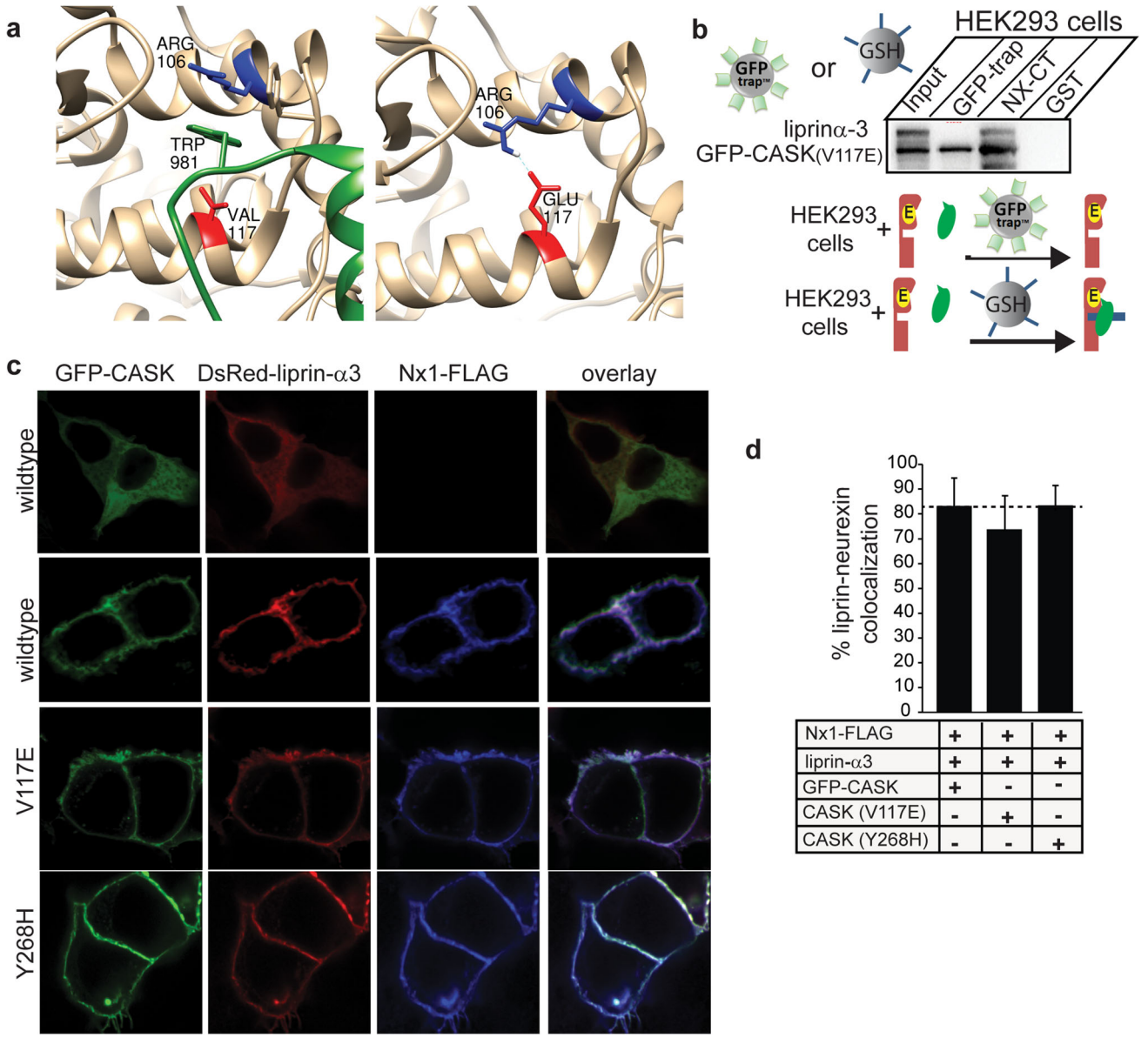

Fig. 5 Liprin-α interacts strongly with the CASK (V117E)–neurexin complex but not with CASK (V117E). **a** Valine 117 (*red*) in CASK (*tan*) is located in a critical location for allowing insertion of the CASK-interacting loop of liprin-α (*green*). Mutation to glutamate at position 117 in CASK (*right panel*) supports formation of a salt bridge with Arg106, based on computational modeling. **b** HEK293 cells were transfected with the mutant GFP-CASK (V117E) and liprin-α3. GFP-CASK was precipitated using either GFP-Trap™ beads or glutathione beads with the GST-tagged cytosolic tail of neurexin attached. Nearly 18 % of CASK from the input was precipitated in both experiments; ~11 % of input liprin-α3 was co-precipitated on neurexin beads, whereas no liprin-α3 was detectable on GFP-Trap™ beads. *Below* the *panel* is a cartoon diagram in which starting material is shown on the *left* of the *arrow* and predominant species pulled down is shown on the *right* of the *arrow*. Pulldown strategy is indicated by *entity* over the *arrow* (GFP-Trap® beads or glutathione beads with NxCT). CASK with V117E mutation, *red* with *yellow*; liprin-α, *green*; NxCT, *blue*. **c** HEK293 cells were plated on poly-lysine-coated coverslips and transiently transfected with cDNA as indicated. Forty-eight hours later, cells were fixed and immunostained with anti-FLAG primary antibody and anti-mouse-Alexa 633 secondary antibody, mounted on slides, and imaged using laser scanning confocal microscopy at ×63. **d** Percent colocalization of liprin-α and membrane-bound Nx1-FLAG from recruitment assays in **c**, quantified using ImageJ (mean and SEM; 20 cells from 3 independent experiments were analyzed for each condition)

some CaM kinases, a salt bridge forms between the V117 equivalent residue (E or D in conventional CaM kinases) and R106 [10]; Fig. 5a); formation of such a salt bridge is presumed to disrupt the hydrophobic pocket into which the liprin-α loop containing the VWV motif inserts, thus blocking the CASK–liprin-α interaction observed in the crystal structure (Figs. 1e, 5a). As described above, immunoprecipitation results suggest that CASK and liprin-

α have two modes of interaction, but it is not clear how much structural overlap there is between these two modes of interaction. We therefore produced a GFP-CASK (V117E) mutation and tested its ability to co-precipitate with liprin-α3 using either GFP-trap® beads (binary complex) or NxCT (ternary complex) from HEK293 cells expressing the CASK mutant and liprin-α3. Both GFP-trap® beads and NxCT beads efficiently precipitated GFP-CASK (V117E) (Fig. 5b). The CASK (V117E) mutant, however, only brings down liprin-α when bound to the neurexin cytosolic tail (Fig. 5b), consistent with the notion that there is a second mode of interaction between CASK and liprin-α; these results indicate that, in the presence of the neurexin cytosolic tail, CASK and liprin-α interact in a manner that does not rely on the hydrophobic pocket of the CASK CaMK domain where V117 is located (Fig. 5a). This alternative interaction site apparently eliminates competition between liprin-α and Mint1 for the same hydrophobic binding pocket on the CaMK domain of CASK, allowing for both proteins to bind to CASK simultaneously (Fig. 4d). A recruitment assay was performed to further demonstrate the ability of the CASK-V117E mutant to bind to liprin-α when complexed with neurexin (Fig. 5c). It has also been proposed that some disease-inducing mutations in CASK may elicit their effects by altering the interaction between CASK and liprin-α [10]. One such mutation, Y268H, is a missense mutation in CASK that has been shown to reduce the affinity of liprins-α for CASK by roughly 2.5 fold [10]. A recruitment assay using GFP-CASK (Y268H) suggests that this mutation does not affect the recruitment of liprin-α to the CASK–neurexin complex (Fig. 5c, d), again emphasizing the existence of a novel mode of interaction that relies primarily on a binding surface created when CASK is bound to neurexin.

Formation of the CASK–liprin-α–neurexin complex is regulated by CASK-dependent neurexin phosphorylation

Since the CASK–neurexin complex mediates liprin-α recruitment and since CASK can phosphorylate neurexin in a synaptic activity-regulated manner [5], we next tested the effect of neurexin phosphorylation on the interaction between CASK and liprin-α. CASK kinase activity is inhibited by divalent ions and thus CASK phosphorylates the cytosolic tail of neurexin in a divalent ion-sensitive manner [5]. Mass spectrometric assessment of phosphorylation in in vitro conditions demonstrated that three serines immediately proximal to the CASK binding motif in neurexin1 get phosphorylated (Online Resource 5). This prompted us to create a neurexin1 cytosolic tail in which the three CASK-phosphorylated serines were mutated to aspartate (NxCT-SD; Fig. 6a), since aspartates are often used as phosphomimetics [32]. Wildtype NxCT and NxCT-SD were then used to precipitate CASK from rat brain. Although CASK itself was efficiently precipitated by both wildtype NxCT and NxCT-SD, there was a dramatic decrease in co-precipitated liprins-α (Fig. 6a, b) when using the NxCT-SD mutant. Quantitative blots of liprin-α1 indicated that liprin-α co-precipitation is reduced by more than 50 % when the neurexin serines are substituted by aspartate (Fig. 6b). To examine this effect in the context of a cell, the recruitment assay was performed with full-length wildtype neurexin1β, a neurexin1β in which the serines of interest were mutated to aspartate (Nx-SD), and a neurexin1β in which the serines of interest were mutated to alanine (Nx-SA), which is phosphorylation-deficient. Consistent with the biochemical experiments, the localization of liprin-α3 with Nx-SD and CASK is reduced (Fig. 6c, d). Some fraction of liprin-α3 still gets recruited since the Nx-SD mutation does not abolish all interaction with liprin-α, as seen in Fig. 6a. The CASK (V117E) mutant even further reduced the amount of neurexin–liprin-α–CASK complex formation (Fig. 6c, d), presumably by eliminating the interaction between a fraction of liprin-α binding to CASK at the CaMK site. The recruitment assay results (Fig. 6c, d) from the phosphorylation-deficient neurexin (Nx-SA) demonstrate that the effects on liprin recruitment are indeed attributable to phosphorylation, since the Nx-SA variant robustly recruited liprin to the membrane.

To directly test the effect of CASK-mediated neurexin phosphorylation on the recruitment of liprins-α, pulldowns from brain lysate were performed under conditions where CASK kinase activity was either activated or inhibited. Glutathione beads to which full-length CASK was bound were incubated with brain lysate either in 10 mM magnesium to inhibit CASK activity completely or with 10 mM ATP and 5 mM EDTA to activate CASK kinase activity [5]. As shown in Fig. 6e, f, co-precipitation of liprin-α3 is impaired in the presence of activated CASK (+ATP and EDTA; neurexin phosphorylation confirmed using ^{32}P phosphorylation assay), but co-precipitation of other CASK binding partners (Mint1, Veli) was not impaired. Together these results (Fig. 6) indicate that CASK-mediated phosphorylation of neurexin1 regulates the interaction of liprins-α with the neurexin–CASK complex.

CASK-dependent phosphorylation destabilizes neurexin

To extend these results to a physiologically relevant system, mixed cortical cultures (DIV 8) expressing tdTomato [25] as a genetic marker for neurons were immunostained for a presynaptic marker, Bassoon [33] and neurexin under

conditions of activity (vehicle-treated) and or pharmacologically-induced inactivity (APV and TTX added overnight to eliminate network activity) (Fig. 7a). Such inactivation has been previously shown to dramatically increase neurexin phosphorylation by CASK due to a reduced influx of divalent ions [5]. Our data indicate that pharmacological inactivation of neuronal network activity decreases the intensity of neurexin immunostaining by approximately 30 % (Fig. 7a, b). To determine whether the reduction in the amount of neurexin was occurring at the transcriptional level, we measured amounts of neurexin1α and β mRNA (antibody used for immunostaining recognizes both isoforms) from these cortical cultures (Fig. 7c). Quantitative real-time PCR data revealed that levels of both neurexin-1β and neurexin-1α mRNA stay constant (Fig. 7d), suggesting that neurexin protein turnover is affected when neurexin phosphorylation increases.

The finding that CASK's phosphorylation of neurexin ultimately reduces overall levels of neurexin in neurons led us to consider previous work in this area. Reduction of CASK expression has been shown to reduce neurexin phosphorylation in neurons [5], so we therefore tested the level of neurexin in a CASK hypomorph mouse brain (Online Resource 7; [4]). Our data indicate that reduction in CASK leads to a reduction in level of neurexins consistent with the previous observation that CASK knockout mice have decreased levels of neurexin [4]. CASK's role in the stabilization of neurexin is seemingly contradictory; although CASK is required to stabilize neurexin, as evinced by the decreased levels of neurexin in CASK knockout mice, an increase in CASK-dependent neurexin phosphorylation seems to enhance neurexin turnover.

In order to confirm these opposing roles of CASK in neurexin stabilization, we examined the effect of overexpressing CASK-4M on neurexin levels. CASK-4M is an engineered variant of CASK [18] that has been converted into a divalent ion-dependent kinase by substitution of four residues in its nucleotide binding pocket (Fig. 7e, f). CASK-4M is capable of phosphorylating neurexin in the presence of divalent ions and is therefore not inhibited by neuronal activity. CASK-deleted neurons were transduced with either wildtype CASK or CASK-4M and levels of neurexin1-β were measured (Fig. 7g, h). Expression of wildtype CASK increases the level of neurexin1-β, but expression of the more active CASK-4M does not increase levels of neurexin1-β (Fig. 7g, h), indicating that CASK-dependent phosphorylation negatively regulates neurexin1-β levels. Liprin-α3 amounts are unchanged by knockout of CASK or expression of CASK-4M (Fig. 7i), indicating that CASK does not affect liprin-α turnover. When considered as a whole, our data indicate that neurexin is stabilized due to its participation in the CASK–liprin–Mint complex described here, and in inactive neurons when CASK is activated and therefore phosphorylates neurexin, liprin can no longer remain associated with the complex, leading to increased neurexin turnover (Fig. 8).

Fig. 6 CASK–liprin-α–neurexin complex formation is regulated by CASK-dependent neurexin phosphorylation. **a** Endogenous CASK complexes were precipitated with the wildtype neurexin cytosolic tail (NX-wt; sequence shown under blot with serines phosphorylated by CASK shown in *red*), neurexin cytosolic tail containing phosphomimetic mutations (NX-SD; sequence shown under blot with aspartate substitutions shown in *red*), or GST. Proteins were blotted using the indicated antibodies. Cartoon diagrams representing the predominant species pulled down with either NX-wt or NX-SD are shown. CASK, *red*; Mint1, *purple*; liprin-α, *green*; neurexin, *blue*; NX-SD, *blue* with *yellow* "SD". **b** Immunoblots were quantified (mean and SEM; $n = 3$; *asterisk* indicates significance of $p < 0.05$). **c** HEK293 cells were plated on poly-lysine-coated coverslips and transiently transfected with cDNA for GFP-CASK, liprin-α3, wildtype neurexin1β, neurexin1β with serine-to-aspartate mutations (NX-SD), and neurexin1β with serine-to-alanine mutations (NX-SA), as indicated. Forty-eight hours later, cells were fixed and immunostained with anti-FLAG primary antibody and anti-mouse-Alexa 633 secondary antibody, mounted on slides, and imaged using laser scanning confocal microscopy at ×63. *Scale bar* is 10 µm. **d** Percent colocalization of liprin-α3 and membrane-bound Nx1-FLAG from recruitment assays in **c** were quantified using ImageJ (mean and SEM; 20 cells from 3 independent experiments were analyzed for each condition; *asterisk* indicates significance of $p < 0.05$). **e** GST pull-down from brain lysate using full-length GST-CASK on glutathione beads was performed with ATP (10 mM ATP plus 5 mM EDTA) to activate CASK kinase activity or without ATP (5 mM $MgCl_2$) to inhibit CASK kinase activity. Proteins were blotted with indicated antibodies (*upper panel* Ponceau S staining; *middle panel* blots; *bottom panel* neurexin phosphorylation assay with ATP[γ-^{32}P]). **f** Quantification of band intensity levels from **e**, showing differences in the percent of input liprin and Velis brought down by the CASK complex in the presence or absence of ATP (mean and SEM; $n = 3$; *asterisk* indicates significance of $p < 0.05$). Cartoon diagrams representing the predominant species pulled down in the presence or absence of ATP are shown. CASK, *red*; Mint1, *purple*; liprin-α, *green*; neurexin, *blue*; phosphorylation indicated by *yellow star*

Discussion

CASK was one of the first presynaptic scaffolding proteins to be described [13], and ablation of the gene in mice has shown it to be essential for survival after birth [4]. Nevertheless the precise function of CASK and in particular its synaptic function has still not been resolved; although some studies have focused on a role for CASK in synaptogenesis, others suggest CASK is primarily a trafficking molecule and may not play a role in synaptogenesis [4, 34]. Analyses of CASK mutant mice suggest that CASK expression is essential, but that loss of CASK does not affect typical neuronal properties such as membrane excitability, calcium-dependent presynaptic release or postsynaptic receptor localization [4]. CASK is known to interact with several other molecules including kinases (CDK5 [12], CaMKII [35], PKC-ε [36], PKA [37]), ion

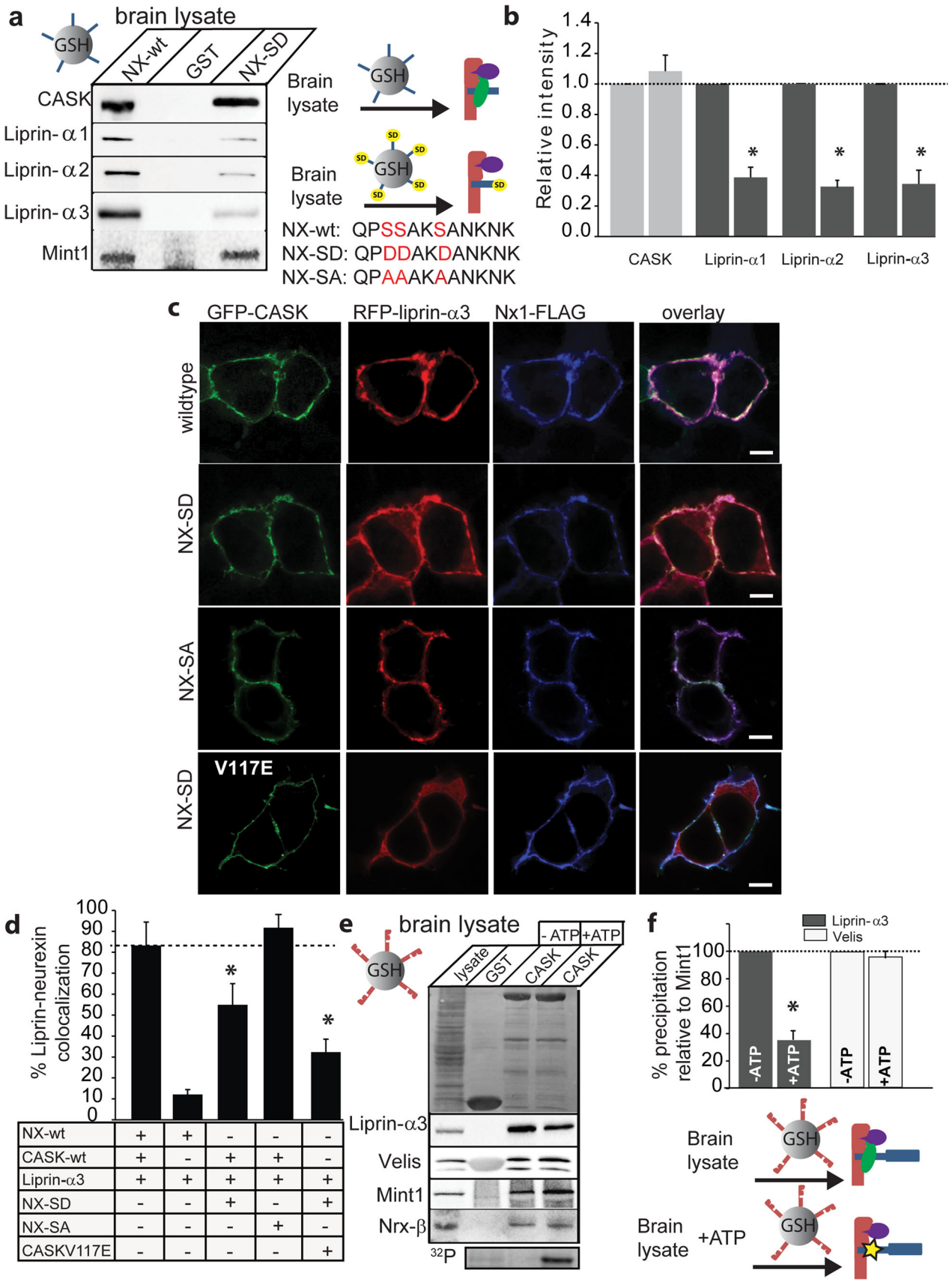
a
brain lysate
GSH
NX-wt
GST
NX-SD
CASK
Liprin-α1
Liprin-α2
Liprin-α3
Mint1
Brain lysate
Brain lysate
NX-wt: QPSSAKSANKNK
NX-SD: QPDDAKDANKNK
NX-SA: QPAAAKAANKNK
b
Relative intensity
CASK
Liprin-α1
Liprin-α2
Liprin-α3
c
GFP-CASK
RFP-liprin-α3
Nx1-FLAG
overlay
wildtype
NX-SD
NX-SA
NX-SD
V117E
d
% Liprin-neurexin colocalization
NX-wt
CASK-wt
Liprin-α3
NX-SD
NX-SA
CASKV117E
e
brain lysate
- ATP
+ATP
lysate
GST
CASK
CASK
Liprin-α3
Velis
Mint1
Nrx-β
32P
f
Liprin-α3
Velis
% precipitation relative to Mint1
-ATP
+ATP
-ATP
+ATP
Brain lysate
Brain lysate
+ATP
GSH

channels (calcium ion channel [38], Kir2.1 [39], ether-a-go-go [40], calcium pump 4B/Cl [41]), regulatory proteins (calmodulin [3], rabphilin [42], RGS4 [36]), ubiquitin ligases (Parkin [43]), transcription activators (Tbr-1 [44], Id1 [45]), adhesion molecules (neurexin [3], syndecan [46], SynCAM [47], JAM-1 [48], Neph1 and 2 [49]), other scaffolding molecules (Mint1 [13], Veli [13], Dlg, SAP97, GRIP1 [36]), cytoskeletal coupling molecules (protein 4.1 [46], FRMD7 [50] BCl11A/CTIP1 [51]) and the gap junction protein connexin-43 [52].

In this study, we focused on CASK's interaction with three of the above-mentioned binding partners: Mint1, liprin-α, and neurexin1β. Like CASK, the set of proteins known as neurexins are associated with neurodevelopmental defects such as autism [53, 54], schizophrenia [55] and mental retardation [56, 57]. Neurexins are known to be adhesion molecules, and in vitro studies have suggested that neurexins are the major presynaptic adhesion molecules involved in synaptogenesis [58]. In vivo studies, however, have failed to confirm this role, and it has been suggested instead that neurexins alter the properties of the synapse [59]. Liprins-α are synaptic proteins with an evolutionarily conserved role in presynaptic active zone formation and function [8, 60, 61]. Liprins-α also may play a role in the formation of actin stress fibers [62] and the targeting of synaptic vesicles to the synapse [63]. Mint1 (also known as X11a) is a scaffolding protein found primarily in neurons and is involved in trafficking of proteins, including ion channels, receptors, and amyloid precursor protein [64]. This group of proteins—CASK, neurexin1β, liprin-α, and Mint1—and their interactions with each other is of particular interest because of their purported importance at the presynapse and because of sometimes contradictory information existing in the literature about the nature of their interactions.

One intriguing discrepancy in the literature surrounds CASK's interaction with Mint1 and liprin-α. It has been well established in pull-down assays [13, 14] from whole brain lysate that CASK and Mint1 interact. The interaction between CASK and liprin-α, however, is not detected in such assays and was only identified indirectly in a pull-down assay using Veli as bait [11]. Efforts to identify a direct interaction between CASK and liprin-α in immunoprecipitation or pull-down assays have been inconsistent. Use of a CASK antibody fails to immunoprecipitate liprin from brain lysate (Fig. 2b), whereas use of GST-CASK immobilized on glutathione beads successfully pulls down liprins-α from brain lysate (Fig. 2e); this strongly suggests that binding of the CASK antibody to its epitope (CASK's L27 domains; Fig. 2a) interferes with formation of the CASK–liprin complex, even though a recently published co-crystal structure of CASK and liprin suggests that only CASK's CAMK domain is required for the interaction [10]. This co-crystal structure (3TAC.pdb) prompted us to look into the possibility that liprin-α and Mint1 can compete for binding to CASK's CaMK domain. Such competition might also help explain why liprin-α is not routinely found when looking for CASK binding partners from pull-down assays. Indeed, our results suggest that, in the presence of Mint1, liprin-α binding to CASK is significantly reduced (Fig. 2c, d). In a surprising twist, this competition between liprin-α and Mint1 for CASK binding is eliminated in the presence of neurexin. In fact, we demonstrate the formation of a multi-protein complex involving CASK, neurexin1β, Mint1, and liprin-α (Fig. 4d), suggesting that although Mint1 and liprin-α indeed compete for binding to CASK's CaMK domain, liprin-α and CASK have a second mode of interaction that is invoked when CASK is bound to the cytoplasmic tail of neurexin1β. The specific structural nature of this second mode of interaction remains to be investigated. It is possible that the formation of the CASK–neurexin complex, which occurs via CASK's PDZ domain, induces a conformational change in CASK that reveals an alternate binding surface, since this interaction occurs via β-sheet augmentation [65]. Another possibility is simply that liprin-α interacts with a surface that includes portions of both neurexin1β and CASK and does not rely on a conformational change.

Fig. 7 Inhibition of neuronal activity destabilizes neurexin protein levels. **a** Mixed mouse cortical cultures (DIV 8) expressing tdTomato (*blue*; used as a neuronal marker and fluorescence fill to clearly delineate neurons in a low-density culture) were either treated with vehicle (control) or 0.5 μM tetrodotoxin (TTX) and 50 μM (2*R*)-amino-5-phosphonovaleric acid (APV) overnight (20 h) to silence all activity. Cells were then fixed and immunostained for Bassoon, a presynaptic marker (*green*), and neurexin1 (*red*), mounted on slides and imaged using laser scanning confocal microscopy at ×63. *Dashed box* indicates region expanded in *lower panel*. *Scale bar* is 20 μm (*upper two panels*) and 2 μm (*lower panel*). **b** Neurexin intensity was quantified by tracing axons and measuring mean pixel intensity along each tracing using the software, Fiji. Bassoon intensity was quantified per synapse and a ratio of neurexin to Bassoon intensity is plotted (mean and SEM; ten images from each of three independent experiments were analyzed; *asterisk* indicates significance of $p < 0.05$). **c** Immunoblot from brain lysate using pan-neurexin antibody indicating the presence of both α and β neurexins (NRX). **d** Relative mRNA levels were assessed in neuronal cultures treated as in **a** using real-time qPCR (mean and SEM; $n = 3$). **e**, **f** CASK (wildtype) nucleotide pocket complexed with 3′AMP in *orange* (3C0H.pdb; [18]) and CASK4M nucleotide binding pocket complexed with AMPPNP in *orange* and Mn^{2+} in *purple* (3MFU.pdb; [18]). The four residues that are critical for conferring the ability to bind divalent ions are indicated in *yellow*. **g** Representative immunoblots from CASK null neuronal cultures transduced with a control virus, virus expressing wildtype CASK (CASK-WT), or mutated CASK (CASK-4M). Antigens for which the blots were probed are indicated. **h** Quantitation of neurexin1β levels normalized to synaptophysin from immunoblots. The statistics were calculated from neuronal cultures done from two different knockout pups, each done in triplicate. **i** Quantitation of liprin-α3 normalized to synaptophysin

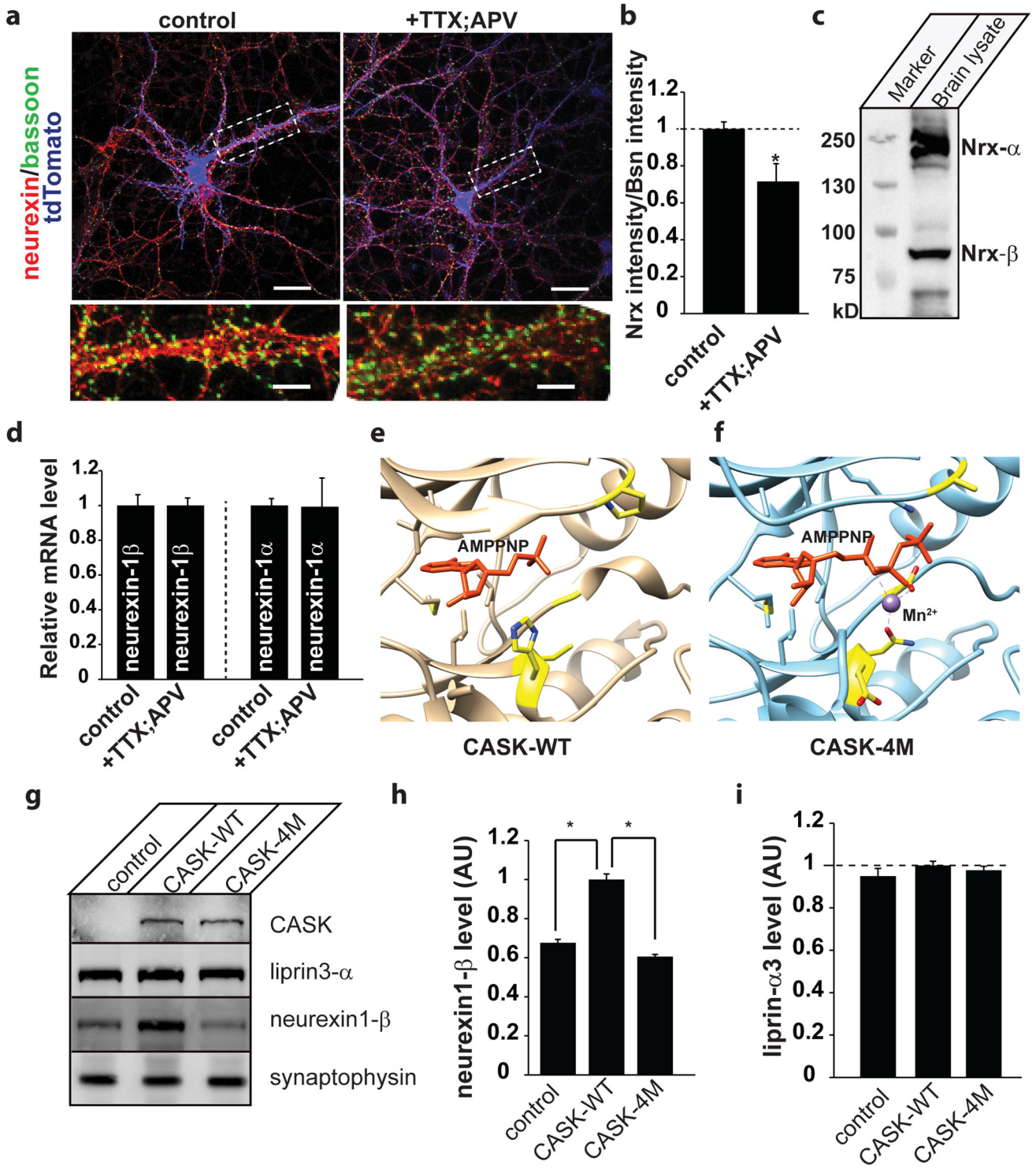
a
control
+TTX;APV
neurexin/bassoon
tdTomato
b
Nrx intensity/Bsn intensity
1.2
1
0.8
0.6
0.4
0.2
0
*
control
+TTX;APV
c
Marker
Brain lysate
250
130
100
75
kD
Nrx-α
Nrx-β
d
Relative mRNA level
1.2
1
0.8
0.6
0.4
0.2
0
neurexin-1β
neurexin-1β
neurexin-1α
neurexin-1α
control
+TTX;APV
control
+TTX;APV
e
AMPPNP
CASK-WT
f
AMPPNP
Mn2+
CASK-4M
g
control
CASK-WT
CASK-4M
CASK
liprin3-α
neurexin1-β
synaptophysin
h
neurexin1-β level (AU)
1.2
1
0.8
0.6
0.4
0.2
0
*
*
control
CASK-WT
CASK-4M
i
liprin-α3 level (AU)
1.2
1
0.8
0.6
0.4
0.2
0
control
CASK-WT
CASK-4M

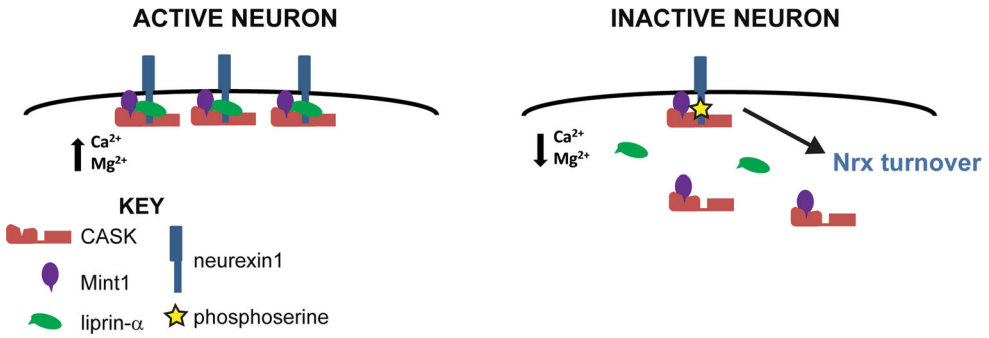

Fig. 8 Model of neurexin stabilization by CASK. In active neurons, when levels of divalent ions are high, neurexin is stabilized by its interaction with CASK and its binding partners. In inactive neurons, when levels of divalent ions decrease, thus activating CASK's kinase activity, CASK phosphorylates neurexin (*yellow star*), which disrupts liprin's interaction with the complex and results in an increase in neurexin turnover. CASK, *red*; Mint1, *purple*; liprin-α, *green*; neurexin, *blue*

Perhaps an even greater challenge than structurally characterizing the multi-protein complex of CASK, neurexin1β, liprin-α and Mint1 is placing this complex into its appropriate functional context. CASK was originally classified as a pseudokinase, however it was recently demonstrated that CASK is a specialized kinase which is not only magnesium-independent but is actually inhibited by divalent ions [5, 18]. This sensitivity to divalent ions offers a novel regulatory control mechanism for CASK-mediated phosphorylation of neurexins. Although the physiological significance of neurexin phosphorylation has not yet been solidified, an alignment of the sequences associated with the cytosolic tails of three rat neurexins and a related region of the protein SynCAM, another synaptogenic adhesion molecule known to interact with CASK [47], reveals striking conservation in the region of each protein that interacts with CASK, despite the lack of overall conservation (Online Resource 6). We speculate that the divergent regions of the cytosolic tails are responsible for differential signal transduction mediated by these molecules. Of interest is the fact that the SynCAM tail has aspartates arranged in a manner similar to the serines in neurexin1 that are targets of CASK phosphorylation, which parallels our use of the serine-to-aspartate NxSD mutant to mimic a phosphorylated state [32]. Since CASK is an extremely slow kinase, the phosphorylation status of neurexin is sustained by its stoichiometric interaction with CASK rather than rapid enzymatic turnover. When divalent ion levels are low, such as would be the case in neurons with extremely low levels of activity, neurexin phosphorylation by CASK is maintained, but in active neurons when concentrations of divalent ions, particularly Ca^{2+}, can become quite high during voltage-gated ion channel opening in response to action potentials, CASK kinase activity is inhibited, and neurexin phosphorylation levels decrease. Our data suggest that when neurexin is not phosphorylated, the CASK–neurexin–Mint1 complex is more likely to associate with the active zone protein liprin-α. In neuronal culture, levels of immunostained neurexin in untreated culture are higher than levels from cultures treated with TTX and APV (Fig. 7a,), suggesting that the association of liprin-α with the CASK–neurexin complex in active neurons stabilizes this complex at the plasma membrane. A relationship between CASK and neurexin levels was first noted in the CASK knockout mouse [4], where it was observed that levels of neurexin1β were 70 % of the levels seen in wildtype mice. CASK thus seems to play a Janus-faced role in the stabilization of neurexin; although it is required to stabilize neurexin, as shown by the reduced levels seen in knockout mice, an increase in CASK-dependent neurexin phosphorylation seems to enhance neurexin turnover. Combining the results from this study with the observation of neurexin levels in the CASK knockout mouse, we propose that CASK plays a critical structural role as an adaptor protein linking neurexin to liprin, which stabilizes neurexin levels. We have confirmed that this stabilization of neurexin is sensitive to CASK-dependent phosphorylation by expressing CASK-4M, which is stimulated rather than inhibited by divalent ions. Overexpression of CASK is able to upregulate neurexin as expected, but overexpression of CASK-4M is incapable of doing so. Thus in addition to its scaffolding role, CASK plays a key regulatory role in maintaining neurexin in complex with the active zone organizer liprin-α in active neurons but destabilizes the interaction of neurexin and liprin in periods of neuronal inactivity, leading to an overall decrease in neurexin levels (Fig. 8). Another recent study concludes that the turnover rate of neurexin1β is increased in inactive neurons, in agreement with what is shown in this work [66].

Understanding CASK's regulation of the formation of a complex composed of important presynaptic proteins—neurexin1β, Mint1, and liprin-α—is an important step towards understanding activity-dependent biochemical

changes. Further work is clearly needed to tease apart the complicated nature of these multi-protein complexes and what regulates their formation, but our findings represent a first step toward defining a role for CASK kinase activity in regulating the formation of a large protein complex present at the active zone.

Acknowledgments This work was partially supported by NIH award 1R01EY024712-01A1 to KM. This work was supported by a start-up package to KM from VTCRI. Work in S.S.'s laboratory is supported by the Deutsche Forschungsgemeinschaft (DFG, SFB1089), the German Ministry of Research and Education (BMBF, 01GQ0806), and local funding (BONFOR). S.S. would like to thank Verena Borm and Lioba Dammer for excellent technical assistance. The authors would like to thank Dr. Thomas Südhof for sharing the Mint1 plasmid and liprin-α antibody 4396.

Compliance with ethical standards

Ethical standards The experiments contained herein comply with the current laws of the countries in which they were performed.

Conflict of interest The authors declare that they have no conflict of interest.

References

1. Sudhof TC (2012) The presynaptic active zone. Neuron 75(1):11–25. doi:10.1016/j.neuron.2012.06.012
2. Schoch S, Gundelfinger ED (2006) Molecular organization of the presynaptic active zone. Cell Tissue Res 326(2):379–391. doi:10.1007/s00441-006-0244-y
3. Hata Y, Butz S, Sudhof TC (1996) CASK: a novel dlg/PSD95 homolog with an N-terminal calmodulin-dependent protein kinase domain identified by interaction with neurexins. J Neurosci 16(8):2488–2494
4. Atasoy D, Schoch S, Ho A, Nadasy KA, Liu X, Zhang W, Mukherjee K, Nosyreva ED, Fernandez-Chacon R, Missler M, Kavalali ET, Sudhof TC (2007) Deletion of CASK in mice is lethal and impairs synaptic function. Proc Natl Acad Sci USA 104(7):2525–2530. doi:10.1073/pnas.0611003104
5. Mukherjee K, Sharma M, Urlaub H, Bourenkov GP, Jahn R, Sudhof TC, Wahl MC (2008) CASK Functions as a Mg^{2+}-independent neurexin kinase. Cell 133(2):328–339. doi:10.1016/j.cell.2008.02.036
6. Ko J, Na M, Kim S, Lee JR, Kim E (2003) Interaction of the ERC family of RIM-binding proteins with the liprin-alpha family of multidomain proteins. J Biol Chem 278(43):42377–42385. doi:10.1074/jbc.M307561200
7. Schoch S, Castillo PE, Jo T, Mukherjee K, Geppert M, Wang Y, Schmitz F, Malenka RC, Sudhof TC (2002) RIM1alpha forms a protein scaffold for regulating neurotransmitter release at the active zone. Nature 415(6869):321–326. doi:10.1038/415321a
8. Kaufmann N, DeProto J, Ranjan R, Wan H, Van Vactor D (2002) Drosophila liprin-alpha and the receptor phosphatase Dlar control synapse morphogenesis. Neuron 34(1):27–38. pii: S0896627302006438
9. Zhen M, Jin Y (1999) The liprin protein SYD-2 regulates the differentiation of presynaptic termini in *C. elegans*. Nature 401(6751):371–375. doi:10.1038/43886
10. Wei Z, Zheng S, Spangler SA, Yu C, Hoogenraad CC, Zhang M (2011) Liprin-mediated large signaling complex organization revealed by the liprin-alpha/CASK and liprin-alpha/liprin-beta complex structures. Mol Cell 43(4):586–598. doi:10.1016/j.molcel.2011.07.021
11. Olsen O, Moore KA, Fukata M, Kazuta T, Trinidad JC, Kauer FW, Streuli M, Misawa H, Burlingame AL, Nicoll RA, Bredt DS (2005) Neurotransmitter release regulated by a MALS-liprin-alpha presynaptic complex. J Cell Biol 170(7):1127–1134. doi:10.1083/jcb.200503011
12. Samuels BA, Hsueh YP, Shu T, Liang H, Tseng HC, Hong CJ, Su SC, Volker J, Neve RL, Yue DT, Tsai LH (2007) Cdk5 promotes synaptogenesis by regulating the subcellular distribution of the MAGUK family member CASK. Neuron 56(5):823–837. doi:10.1016/j.neuron.2007.09.035
13. Butz S, Okamoto M, Sudhof TC (1998) A tripartite protein complex with the potential to couple synaptic vesicle exocytosis to cell adhesion in brain. Cell 94(6):773–782. pii: S0092-8674(00)81736-5
14. Tabuchi K, Biederer T, Butz S, Sudhof TC (2002) CASK participates in alternative tripartite complexes in which Mint 1 competes for binding with caskin 1, a novel CASK-binding protein. J Neurosci 22(11):4264–4273
15. Stafford RL, Ear J, Knight MJ, Bowie JU (2011) The molecular basis of the Caskin1 and Mint1 interaction with CASK. J Mol Biol 412(1):3–13. doi:10.1016/j.jmb.2011.07.005
16. Pernhorst K, Raabe A, Niehusmann P, van Loo KM, Grote A, Hoffmann P, Cichon S, Sander T, Schoch S, Becker AJ (2011) Promoter variants determine gamma-aminobutyric acid homeostasis-related gene transcription in human epileptic hippocampi. J Neuropathol Exp Neurol 70(12):1080–1088. doi:10.1097/NEN.0b013e318238b9af
17. Mosedale M, Egodage S, Calma RC, Chi NW, Chessler SD (2012) Neurexin-1alpha contributes to insulin-containing secretory granule docking. J Biol Chem 287(9):6350–6361. doi:10.1074/jbc.M111.299081
18. Mukherjee K, Sharma M, Jahn R, Wahl MC, Sudhof TC (2010) Evolution of CASK into a Mg^{2+}-sensitive kinase. Sci Signal 3(119):ra33. doi:10.1126/scisignal.2000800
19. Calcium phosphate-mediated transfection of eukaryotic cells (2005). Nat Methods 2(4):319–320. doi:10.1038/nmeth0405-319
20. Zurner M, Mittelstaedt T, tom Dieck S, Becker A, Schoch S (2011) Analyses of the spatiotemporal expression and subcellular localization of liprin-alpha proteins. J Comp Neurol 519(15):3019–3039. doi:10.1002/cne.22664
21. Brusca JS, Radolf JD (1994) Isolation of integral membrane proteins by phase partitioning with Triton X-114. Methods Enzymol 228:182–193
22. Pettersen EF, Goddard TD, Huang CC, Couch GS, Greenblatt DM, Meng EC, Ferrin TE (2004) UCSF Chimera–a visualization system for exploratory research and analysis. J Comput Chem 25(13):1605–1612. doi:10.1002/jcc.20084
23. Sali A, Blundell TL (1993) Comparative protein modelling by satisfaction of spatial restraints. J Mol Biol 234(3):779–815. doi:10.1006/jmbi.1993.1626
24. Dunbrack RL Jr (2002) Rotamer libraries in the 21st century. Curr Opin Struct Biol 12(4):431–440
25. Chavan V, Willis J, Walker SK, Clark HR, Liu X, Fox MA, Srivastava S, Mukherjee K (2015) Central presynaptic terminals are enriched in ATP but the majority lack mitochondria. PLoS One 10(4):e0125185. doi:10.1371/journal.pone.0125185
26. Zhu Y, Romero MI, Ghosh P, Ye Z, Charnay P, Rushing EJ, Marth JD, Parada LF (2001) Ablation of NF1 function in neurons induces abnormal development of cerebral cortex and reactive gliosis in the brain. Genes Dev 15(7):859–876. doi:10.1101/gad.862101
27. Tiscornia G, Singer O, Verma IM (2006) Production and purification of lentiviral vectors. Nat Protoc 1(1):241–245. doi:10.1038/nprot.2006.37

28. Zurner M, Schoch S (2009) The mouse and human Liprin-alpha family of scaffolding proteins: genomic organization, expression profiling and regulation by alternative splicing. Genomics 93(3):243–253. doi:10.1016/j.ygeno.2008.10.007
29. John B, Sali A (2003) Comparative protein structure modeling by iterative alignment, model building and model assessment. Nucleic Acids Res 31(14):3982–3992
30. Mukherjee K, Slawson JB, Christmann BL, Griffith LC (2014) Neuron-specific protein interactions of Drosophila CASK-beta are revealed by mass spectrometry. Front Mol Neurosci 7:58. doi:10.3389/fnmol.2014.00058
31. Bordier C (1981) Phase separation of integral membrane proteins in Triton X-114 solution. J Biol Chem 256(4):1604–1607
32. Pearlman SM, Serber Z, Ferrell JE Jr (2011) A mechanism for the evolution of phosphorylation sites. Cell 147(4):934–946. doi:10.1016/j.cell.2011.08.052
33. Juranek J, Mukherjee K, Rickmann M, Martens H, Calka J, Sudhof TC, Jahn R (2006) Differential expression of active zone proteins in neuromuscular junctions suggests functional diversification. Eur J Neurosci 24(11):3043–3052. doi:10.1111/j.1460-9568.2006.05183.x
34. Gokce O, Sudhof TC (2013) Membrane-tethered monomeric neurexin LNS-domain triggers synapse formation. J Neurosci 33(36):14617–14628. doi:10.1523/JNEUROSCI.1232-13.2013
35. Lu CS, Hodge JJ, Mehren J, Sun XX, Griffith LC (2003) Regulation of the Ca2 +/CaM-responsive pool of CaMKII by scaffold-dependent autophosphorylation. Neuron 40 (6):1185-1197. pii: S0896627303007864
36. Hong CJ, Hsueh YP (2006) CASK associates with glutamate receptor interacting protein and signaling molecules. Biochem Biophys Res Commun 351(3):771–776. doi:10.1016/j.bbrc.2006.10.113
37. Huang TN, Chang HP, Hsueh YP (2010) CASK phosphorylation by PKA regulates the protein-protein interactions of CASK and expression of the NMDAR2b gene. J Neurochem 112(6):1562–1573. doi:10.1111/j.1471-4159.2010.06569.x
38. Maximov A, Sudhof TC, Bezprozvanny I (1999) Association of neuronal calcium channels with modular adaptor proteins. J Biol Chem 274(35):24453–24456
39. Olsen O, Liu H, Wade JB, Merot J, Welling PA (2002) Basolateral membrane expression of the Kir 2.3 channel is coordinated by PDZ interaction with Lin-7/CASK complex. Am J Physiol Cell Physiol 282(1):C183–C195. doi:10.1152/ajpcell.00249.2001
40. Marble DD, Hegle AP, Snyder ED 2nd, Dimitratos S, Bryant PJ, Wilson GF (2005) Camguk/CASK enhances Ether-a-go-go potassium current by a phosphorylation-dependent mechanism. J Neurosci 25(20):4898–4907. doi:10.1523/JNEUROSCI.4566-04.2005
41. Schuh K, Uldrijan S, Gambaryan S, Roethlein N, Neyses L (2003) Interaction of the plasma membrane Ca^{2+} pump 4b/CI with the Ca^{2+}/calmodulin-dependent membrane-associated kinase CASK. J Biol Chem 278(11):9778–9783. doi:10.1074/jbc.M212507200
42. Zhang Y, Luan Z, Liu A, Hu G (2001) The scaffolding protein CASK mediates the interaction between rabphilin3a and beta-neurexins. FEBS Lett 497(2–3):99–102. pii: S0014-5793(01)02450-4
43. Fallon L, Moreau F, Croft BG, Labib N, Gu WJ, Fon EA (2002) Parkin and CASK/LIN-2 associate via a PDZ-mediated interaction and are co-localized in lipid rafts and postsynaptic densities in brain. J Biol Chem 277(1):486–491. doi:10.1074/jbc.M109806200
44. Hsueh YP, Wang TF, Yang FC, Sheng M (2000) Nuclear translocation and transcription regulation by the membrane-associated guanylate kinase CASK/LIN-2. Nature 404(6775):298–302. doi:10.1038/35005118
45. Qi J, Su Y, Sun R, Zhang F, Luo X, Yang Z (2005) CASK inhibits ECV304 cell growth and interacts with Id1. Biochem Biophys Res Commun 328(2):517–521. doi:10.1016/j.bbrc.2005.01.014
46. Cohen AR, Woods DF, Marfatia SM, Walther Z, Chishti AH, Anderson JM (1998) Human CASK/LIN-2 binds syndecan-2 and protein 4.1 and localizes to the basolateral membrane of epithelial cells. J Cell Biol 142(1):129–138
47. Biederer T, Sara Y, Mozhayeva M, Atasoy D, Liu X, Kavalali ET, Sudhof TC (2002) SynCAM, a synaptic adhesion molecule that drives synapse assembly. Science 297(5586):1525–1531. doi:10.1126/science.1072356
48. Aravindan RG, Fomin VP, Naik UP, Modelski MJ, Naik MU, Galileo DS, Duncan RL, Martin-Deleon PA (2012) CASK interacts with PMCA4b and JAM-A on the mouse sperm flagellum to regulate Ca^{2+} homeostasis and motility. J Cell Physiol 227(8):3138–3150. doi:10.1002/jcp.24000
49. Gerke P, Benzing T, Hohne M, Kispert A, Frotscher M, Walz G, Kretz O (2006) Neuronal expression and interaction with the synaptic protein CASK suggest a role for Neph1 and Neph2 in synaptogenesis. J Comp Neurol 498(4):466–475. doi:10.1002/cne.21064
50. Watkins RJ, Patil R, Goult BT, Thomas MG, Gottlob I, Shackleton S (2013) A novel interaction between FRMD7 and CASK: evidence for a causal role in idiopathic infantile nystagmus. Hum Mol Genet 22(10):2105–2118. doi:10.1093/hmg/ddt060
51. Kuo TY, Hong CJ, Chien HL, Hsueh YP (2010) X-linked mental retardation gene CASK interacts with Bcl11A/CTIP1 and regulates axon branching and outgrowth. J Neurosci Res 88(11):2364–2373. doi:10.1002/jnr.22407
52. Marquez-Rosado L, Singh D, Rincon-Arano H, Solan JL, Lampe PD (2012) CASK (LIN2) interacts with Cx43 in wounded skin and their coexpression affects cell migration. J Cell Sci 125(Pt 3):695–702. doi:10.1242/jcs.084400
53. Kim HG, Kishikawa S, Higgins AW, Seong IS, Donovan DJ, Shen Y, Lally E, Weiss LA, Najm J, Kutsche K, Descartes M, Holt L, Braddock S, Troxell R, Kaplan L, Volkmar F, Klin A, Tsatsanis K, Harris DJ, Noens I, Pauls DL, Daly MJ, MacDonald ME, Morton CC, Quade BJ, Gusella JF (2008) Disruption of neurexin 1 associated with autism spectrum disorder. Am J Hum Genet 82(1):199–207. doi:10.1016/j.ajhg.2007.09.011
54. Feng J, Schroer R, Yan J, Song W, Yang C, Bockholt A, Cook EH Jr, Skinner C, Schwartz CE, Sommer SS (2006) High frequency of neurexin 1beta signal peptide structural variants in patients with autism. Neurosci Lett 409(1):10–13. doi:10.1016/j.neulet.2006.08.017
55. Gauthier J, Siddiqui TJ, Huashan P, Yokomaku D, Hamdan FF, Champagne N, Lapointe M, Spiegelman D, Noreau A, Lafreniere RG, Fathalli F, Joober R, Krebs MO, DeLisi LE, Mottron L, Fombonne E, Michaud JL, Drapeau P, Carbonetto S, Craig AM, Rouleau GA (2011) Truncating mutations in NRXN2 and NRXN1 in autism spectrum disorders and schizophrenia. Hum Genet 130(4):563–573. doi:10.1007/s00439-011-0975-z
56. Bermudez-Wagner K, Jeng LJ, Slavotinek AM, Sanford EF (2013) 2p16.3 microdeletion with partial deletion of the neurexin-1 gene in a female with developmental delays, short stature, and a congenital diaphragmatic hernia. Clin Dysmorphol 22(1):22–24. doi:10.1097/MCD.0b013e32835b8df2
57. Ching MS, Shen Y, Tan WH, Jeste SS, Morrow EM, Chen X, Mukaddes NM, Yoo SY, Hanson E, Hundley R, Austin C, Becker RE, Berry GT, Driscoll K, Engle EC, Friedman S, Gusella JF, Hisama FM, Irons MB, Lafiosca T, LeClair E, Miller DT, Neessen M, Picker JD, Rappaport L, Rooney CM, Sarco DP, Stoler JM, Walsh CA, Wolff RR, Zhang T, Nasir RH, Wu BL (2010) Deletions of NRXN1 (neurexin-1) predispose to a wide

spectrum of developmental disorders. Am J Med Genet B Neuropsychiatr Genet 153B(4):937–947. doi:10.1002/ajmg.b.31063
58. Nam CI, Chen L (2005) Postsynaptic assembly induced by neurexin–neuroligin interaction and neurotransmitter. Proc Natl Acad Sci USA 102(17):6137–6142. doi:10.1073/pnas.0502038102
59. Sudhof TC (2008) Neuroligins and neurexins link synaptic function to cognitive disease. Nature 455(7215):903–911. doi:10.1038/nature07456
60. Spangler SA, Schmitz SK, Kevenaar JT, de Graaff E, de Wit H, Demmers J, Toonen RF, Hoogenraad CC (2013) Liprin-alpha2 promotes the presynaptic recruitment and turnover of RIM1/CASK to facilitate synaptic transmission. J Cell Biol 201(6):915–928. doi:10.1083/jcb.201301011
61. Dai Y, Taru H, Deken SL, Grill B, Ackley B, Nonet ML, Jin Y (2006) SYD-2 Liprin-alpha organizes presynaptic active zone formation through ELKS. Nat Neurosci 9(12):1479–1487. doi:10.1038/nn1808
62. Sakamoto S, Ishizaki T, Okawa K, Watanabe S, Arakawa T, Watanabe N, Narumiya S (2012) Liprin-alpha controls stress fiber formation by binding to mDia and regulating its membrane localization. J Cell Sci 125(Pt 1):108–120. doi:10.1242/jcs.087411
63. Miller KE, DeProto J, Kaufmann N, Patel BN, Duckworth A, Van Vactor D (2005) Direct observation demonstrates that Liprin-alpha is required for trafficking of synaptic vesicles. Curr Biol 15(7):684–689. doi:10.1016/j.cub.2005.02.061
64. Rogelj B, Mitchell JC, Miller CC, McLoughlin DM (2006) The X11/Mint family of adaptor proteins. Brain Res Rev 52(2):305–315. doi:10.1016/j.brainresrev.2006.04.005
65. Daniels DL, Cohen AR, Anderson JM, Brunger AT (1998) Crystal structure of the hCASK PDZ domain reveals the structural basis of class II PDZ domain target recognition. Nat Struct Biol 5(4):317–325
66. Fu Y, Huang ZJ (2010) Differential dynamics and activity-dependent regulation of alpha- and beta-neurexins at developing GABAergic synapses. Proc Natl Acad Sci USA 107(52):22699–22704. doi:10.1073/pnas.1011233108